粒子 - ガンマ線相関を用いた
重イオン共鳴の分子的構造の分析

(課題番号　12640250)

平成 12 年度－平成 14 年度

科学研究費補助金（基盤研究(C)(2)）

研究成果報告書

平成１６年３月

研究代表者　　上　柿　英　二

(秋田大学工学資源学部教授)

Akita University

はしがき

本報告書は平成12年度—平成14年度日本学術振興会科学研究費補助金（基盤研究(C)(2)）の助成を受けた研究課題「粒子-ガンマ線相関を用いた重イオン共鳴の分子的構造の分析」について研究成果をまとめたものである．

著者たちは $^{24}Mg + ^{24}Mg$ ，$^{28}Si + ^{28}Si$ などの比較的重い重イオン衝突でクーロンバリアーを超えるエネルギー領域に観測されている幅の狭い高励起，高スピン共鳴状態の構造と反応機構について，二原子核分子の形成とそれに伴う振動モード励起を考える立場から解明しようとしてきた．この共鳴では，強い遠心力の効果のために二原子核は少し離れて融合しきらず，それでもなお，核間相互作用によって結合を保つような幾何学的配位が支配的になると予想される．この描像は，$^{12}C + ^{12}C$，$^{12}C + ^{16}O$ 共鳴などで明らかに成った double resonance mechanism と著しく異なっているが，^{24}Mg 核や ^{28}Si 核の基底回転帯のメンバーの小さい励起エネルギーは数多くの二原子核配位が同時に競合する事を可能にしていて，そのためにこの様な準安定な幾何学的配位が実現すると思われる．そこで著者らは強結合的描像の「新しい分子的模型」を提案し，以前の二度にわたる科学研究費の補助のもとに，これらの共鳴における二原子核の動力学と共鳴機構の解明を進めてきた．研究開始当初には実験データが乏しく，非弾性散乱の励起関数と $^{24}Mg + ^{24}Mg$ のスピンアラインメントに関するもの程度であったので，非弾性チャンネルへの部分崩壊幅の分析によって理論の検証を試みたが，詳細な分析を行うには限界があった．

最近，ストラスブールで EUROGAM II を用いて $^{28}Si + ^{28}Si$ の「粒子-粒子-ガンマ線相関実験」が実施され，より詳細で非常に興味深いスピンアラインメントの情報が得られた．実験結果の示唆するところでは，共鳴状態を構成する ^{28}Si 核のスピンが反応面に平行で，主に”m＝0”状態になっているらしいのである．この実験結果をもとに，$^{28}Si + ^{28}Si$ 共鳴の構造を明らかにしようとするのが，本研究課題である．課題の遂行にあたってガンマ線強度の生データを提供し，議論してくださった IReS Strasbourg のメンバー，R. Nouicer, C. Beck, F. Haas, R.M. Freeman 博士らに感謝の意を表したい．詳細は概要に譲るが，この分野に少しでも多くの人が関心を持っていただけるならば幸いである．

研究組織

研究代表者　上柿英二（秋田大学　工学資源学部　教授）

研究分担者　阿部恭久（京都大学　基礎物理学研究所　助教授）

研 究 発 表

(1) 学術誌等

1) L. Plagnue, J. Daligault, K. Yabana, T. Tazawa, C. Guet and Y.Abe
Semiclassical versus Quantal Time -Dependent Mean-Field Descriptions of Electron Dynamics in Ion-Cluster Collisions
Phys. Rev. **A61** (2000) 33201-33207.

2) F. Wang, F.S. Zhang and Y. Abe
Pseudorotating Na_4 at finite temperature : tight-binding molecular dynamics studies
Chem.Phys. Lett. **326** (2000) pp. 461-467.

3) S. Ayik and Y. Abe
Stochastic One-Body Transport and Coupling to Mean-Field Fluctuations
Phys. Rev. **C64** (2001) 4609-1, 10.

(2) 国際会議発表・報告集

1) E. Uegaki and Y. Abe
Spin Alignment in Heavy-Ion Resonances, *invited talk*
Proc. of the 7th Intern. Conf. on Clustering Aspects of Nuclear Structure and Dynamics (Rab, Croatia, 14∼16 June 1999), Eds. M. Korolija, Z. Basrak and R. Caplar, (World Scientific, 2000) pp. 160∼165.

2) E. Uegaki and Y. Abe
Angular Correlations in $^{28}Si + ^{28}Si$ Resonances, *invited talk*
Proc. of the Symposium on Nuclaer Clusters: From Light Exotic to Superheavy Nuclei (Rauischholzhausen, Germany, 5∼9 Aug. 2002), Eds. R. Jolos and W. Scheid, (EP Systema, Hungary, 2003) pp. 163∼170.

研 究 成 果 の 概 要

目 次

I. 要 約

重イオン間の共鳴現象は1960年代より知られており，$^{12}C + ^{12}C$ 系では数多くの共鳴準位が発見されてきた．1980年代には，^{24}Mg や ^{28}Si の様なより重い原子核間の衝突に於いても驚くほど幅の狭い，すなわち，寿命の長い共鳴が高スピン状態として複合核の６０ MeV 程度の高励起エネルギー領域に発見されている．これらの共鳴は非弾性チャンネルへ強く崩壊し，その励起関数間には顕著な相関がみられるので，複合核を形成していると思われる．これまで，より軽い $^{12}C + ^{12}C$ や $^{12}C + ^{16}O$ 系については Band-Crossing Model が成功を納めた．すなわち，構成原子核の集団運動励起に伴って，その核スピンと軌道角運動量とが揃った状態が弾性チャンネルと結びつき，共鳴現象が引き起こされるとする描像で現象を良く再現できる．(この現象を確認する重要な物理量として，スピンアラインメントがある．) ところが，^{24}Mg や ^{28}Si では，^{12}C に較べて励起エネルギーは 1/3 程度，逆に相対運動の角運動量は数倍も大きいので，弾性チャンネルと結合する分子的配位として特定のものが重要なのではなく，全体でエネルギー的に好まれる配位，つまり，二原子核の相互作用によって強く結合するような幾何学的配位が支配的になると予想される．この様な安定な分子的構造とその安定点の回りでの動力学を記述するため，著者らは強結合的描像に基づく高スピン重イオン共鳴の分子的模型を提案した．この模型では，単に安定な配位をエネルギー的に探るだけでなく，安定点の回りでの構成核の振動や捻れ的回転運動など，様々な励起モードを求めることができる．これらの運動モードの励起状態が数多く存在する事によって，$^{24}Mg + ^{24}Mg$ や $^{28}Si + ^{28}Si$ 系に多数の共鳴が観測されることを説明できると思われる．

この研究では，共鳴状態の物理量を求めて実験データと比較し，新しい分子的模型の妥当性を検証することを目標として，$^{24}Mg + ^{24}Mg$ と $^{28}Si + ^{28}Si$ 系の差異を明らかにすることや，理論で予想されている様々なモードの存在が実験データにおいてどの様に現れて来るかに強い関心を持っている．本研究課題では，$^{28}Si + ^{28}Si$ 分子共鳴状態についての「粒子 - 粒子 - ガンマ角相関データ」を分析した．スピン非整列を示すデータから共鳴状態の構造について一定の結論を得た．分子模型や角相関についての理論的方法は以下の英文レポートを参照して頂きたい．この要約では簡単に結論的部分のみを述べる．

理論的には, 高スピン重イオン共鳴の分子的模型を用いて部分崩壊幅を算出し, R-matrix 散乱振幅から, フラグメントより二次的に放出されるガンマ線強度を計算できる. 実験はスピンベクトルが反応面に平行であることを示すので, この様な特殊な核構造が分子共鳴のどの様な運動モードで起こるかを明らかにした.

スピンベクトルが反応面上に揃う機構としては以下のことが予想された. ^{28}Si + ^{28}Si の安定構造は oblate 変形した ^{28}Si がその赤道面で接している様な配位である. この安定配位では二つのパンケーキが並んで平面に置かれたような形状となるので, 全体的には, 巨大 prolate 変形した非軸対称回転子と見なせる. この様な非軸対称回転子が超高スピンで回転すればモーメント最大となる軸の回りに回転しやすくなり, K-mixing, すなわちウォブリングモードが発現すると予想される. このとき ^{28}Si の対称軸は反応面に垂直となるが, スピンは対称軸に垂直なので反応面上にある. この様な回転モードは分子的基底状態とバタフライモードで可能である. もう一つの可能性はより単純なものである. 2つの ^{28}Si がその重心を結んだ軸の回りに互いに逆回転して捻れるタイプの運動（ツイストモード）で実現され, スピンは相対ベクトルに平行になる.

これら分子的基底状態と励起状態の3ケースについて角相関を検討した結果, 以下の結論を得た. バタフライ励起モードなどの振動励起状態ではスピンベクトルは反応面に平行であるものの, 振動面に垂直な方向に揃いすぎて実験との一致が良くない. また, ツイストモードでは分子軸方向にスピンが揃ってしまい, これも実験と一致しない. ウォブリングしている基底状態では, スピンの向きは反応面上で特定の方向に偏らないので, これが一番妥当である.

II. REPORT

Analysis for Molecular Structures in Heavy-ion Resonances by using Particle-particle-γ Correlations

Abstract

Particle-particle-gamma data from ^{28}Si+^{28}Si molecular resonances was analised. By using R-matrix scattering amplitudes from high-spin molecular model, we can theoretically calculate gamma-ray intensities from the fragments ^{28}Si which are emitted from the resonance decays. The experimental data suggest "$m = 0$" which means the spins vectors of ^{28}Si are on the reaction plane. We studied what molecular normal modes exibits such a special nuclear structure.

Following mechanism has been expected to obtain the spins parallel to the plane; 1. the stable configuration of ^{28}Si + ^{28}Si is expected to be an equator-equator touching configuration, 2. such a stable configuration has a tri-axial deformation, 3. due to extremely high spin rotation(J=38), the total deformed object rotates around the axis of highest moments of inertia, which give rise to K-mixing so called wobbling mode. Then the symmetry axes of two ^{28}Si are perpendicular to the plane, and the spin vectors are on the plane because they are orthogonal to the axes. Such a rotational mode is possible for the molecular ground state and the butterfly and anti-butterfly modes. We have also another mode twisting to obtain non-alignments by simpler mechanism, in which two ^{28}Si spin around the molecular axis in the opposite spin-vector directions. The vectors are parallel to the molecular axis which rotates on the reaction plane.

Comparing theoretical results with the data, we conclude that the molecular ground state with wobbling rotation is a candidate for the resonance structure. The other two are not good candidates by the following reason. In the butterfly mode and the twisting one the spin vectors are parallel to the fragment direction and the beam one, respectively. Even with the spins parallel to the reaction plane, we obtained no "$m = 0$" from too much concentrated vectors to own directions, because "$m = 0$" require "symmetry around z-axis".

§1. Introduction

Intermediate resonances observed in heavy-ion scattering have offered intriguing subjects in nuclear physics. High-spin resonances well above the Coulomb barrier in $^{24}Mg + ^{24}Mg$ and $^{28}Si + ^{28}Si$ systems exhibit very narrow decay widths, with prominent peaks correlated among the elastic and inelastic channels, which suggest rather long lived compound nuclear systems[1].

Betts et al. firstly observed a series of resonance-like enhancements at $\theta_{cm} = 90°$ in elastic scattering of $^{28}Si + ^{28}Si$[2], and then they gave spin asignments of $J = 34 \sim 42$ by the Legendre-fits for the elastic angular distributions[3]. They further closely studied angle-averaged excitation functions for the elastic and inelastic scatterings, and found broad($\Gamma_{cm} \sim 2.5$keV) structures corresponding to the enhancements[4]. The each broad structures is fragmented into several much narrower peaks with widths $\Gamma_{cm} \sim 150$keV and spacing of a few hundred keV as shown in Fig. 1. Zurmuhle et al. studied the $^{24}Mg + ^{24}Mg$ system and found similar but more prominent resonance peaks[5]. Such narrow peaks are correlatingly seen in the single and mutual channel of the both systems, strengths of which are enhanced more than elastic one. The decay widths in the elastic and inelastic channels up to high spin members of ^{24}Mg or ^{28}Si ground band exhaust about 30% of the total widths, whereas those into α-transfer channels are much smaller[6,7]. These enhancements of symmetric-mass decays strongly suggest di-nuclear molecular configurations for the resonance states. It is also noted that the elastic channel widths are rather small, for example, a few keV, which is quite different from high spin resonances in lighter systems such as $^{12}C + ^{12}C$, $^{16}O + ^{16}O$[8].

From viewpoints of nuclear structure studies, one immediately thinks of secondary minima in fission of heavy nuclei, or of superdeformations which have been intensively studied in medium mass nuclei. Actually Bengtsson *et al.* made Nilsson-Strutinsky calculations for Ni isotopes and obtained energy minimum at large deformation, which appears to correspond to a di-nuclear configuration[9]. On the other hand, considering an angular-momentum dominance in such high spin states, Broglia *et al.* studied the stability of di-nuclear systems by the macroscopic model, without taking into account the shell correction[10]. They employed the liquid-drop model with the proximity potential between ions, including their surface oscillations. They obtained stable configurations with the deformed frag-

ments in high spins less than $56\hbar$, for the ^{26}Mg + ^{26}Mg system. Maass and Scheid calculated shell correction energies of the di-nucleus system by the use of two-center-shell model[11]. By adding the correction energies to the liquid-drop energy, they obtained stable configurations for the ^{24}Mg + ^{24}Mg system with $l_{\rm cr}$ being 38. They also studied an oblate-oblate deformed system, chosing ^{12}C + ^{12}C one, but they did not apply the two-center-shell model. In this case, they used a method rather similar to our molecular model. The present authors proposed a di-nuclear molecular model, by which equilibrium geometrical configurations at high spins and normal modes of motion can be described. Under strong influence of high spin centrifugal force, two constituent deformed nuclei favor elongated configurations with a touch at a tip; a pole-to-pole touching configuration and an equator-equator one were found to be the equiribria for ^{24}Mg+^{24}Mg and ^{28}Si+^{28}Si systems, respectively. They obtained normal modes around the equiribria, which are expected to be responsible to the observed resonances[12 - 14].

Recently a new facet of the ^{28}Si+^{28}Si resonances has been explored. ^{28}Si+^{28}Si scattering experiment has been done on the resonance at $E_{\rm c.m.} = 55.8$MeV at IReS Strasbourg[15]. Figure 2 shows those elastic and inelastic angular distributions, where the solid lines in the lower three panels show $L = 38$ Legendre fits. The oscillating pattern in the elastic and inelastic channels 2^+, $(2^+, 2^+)$ are found to be in good agreement with $L = 38$, which suggests $L = J = 38$ dominance in the resonance, namely, *misalignments* of the fragment spins. γ-rays have been also measured with 4π detectors in coincidence with two ^{28}Si fragments detected at $\theta_{cm} = 90°$.[7,15] Those γ-rays are emitted from the fragments of the excited ^{28}Si nuclei etc. when the resonant compound decays. The angular correlation data show characteristic "$m = 0$" pattern for normal to the reaction plane, which suggests fragment spins $\mathbf{I_1}$ and $\mathbf{I_2}$ are on the scattering plane and is consistent with the misalignments observed in the fragment angular distributions. Now, characteristic features of the experiments are summarized as following three points, which is to be explained theoretically; 1. narrow resonance structures correlating among the elastic and inelastic channels, 2. angular distributions in the elastic and inelastic channels, 3. angular correlations between emerging fragments ^{28}Si and gamma-ray emitted from the fragments. The second characteristic indicates a dominance of the partial wave $L = J$. And the third one indicates "m=0" spin orientations of the fragments in the normal to the reaction plane. Thus, the latter two quantities suggest a disalignment between the orbital angular momentum

and the fragment spins. Those features are much different from $^{12}C + ^{12}C$ and $^{24}Mg + ^{24}Mg$ systems which exhibit spin alignments[16,17]. Thus, the data are expected to provide a good test for the model.

The purpose of the present paper is to clarify the structure of high-spin $^{28}Si + ^{28}Si$ resonances. As already mentioned, we obtained normal modes around the equiribrium of the touching configuration of two ^{28}Si, which are expected to be responsible to the observed resonances. With the new angular correlation data, we are now able to select "what mode is really a candidate for the resonance". For this purpose, we have studied reaction mechanism for resonances and have developed an analysis method for "particle-particle-γ angular correlations". By using R-matrix theory, we obtain partial decay widths and collision matrices for the resonances, which give the informations about resonance decays[18]. Considering γ-ray emissions from the decay fragments, i.e., γ-rays from excited ^{28}Si nuclei, we obtain angular correlations, which enable us to compare the molecular model with the experiments[19].

We have also developed our molecular model to include K-mixing. In the previous molecular model calculations, as an approximation, we have assumed good K-quantum number(projection of the total angular momentum on the molecular z'-axis). Of course there are couplings between them by Coriolis terms, and so we know the existence of K-mixings anyhow. Due to a tri-axial shape of the equilibrium configuration, we have low-lying series of K-good levels, which reminds us that the effects may be important. However there are a lot of Coriolis terms, and the calculations for the coupling matrix are not easy. Therefore, to evaluate the coupling effects, we take semiclassical approach, i.e., we consider the whole rotational system with the tri-axial shape of the stable configurations to be an asymmetric rotator which give rise to K-mixings at high spins. It is not a way of quantal calculation for a system with many degrees of freedom, but it gives more intuitive understanding for the rotational motions of the whole system. Consequently the rotational motions of the tri-axial deformed system are found to be indispensably important for understanding "$m = 0$" dominance of the ^{28}Si spin state, which brings novel aspects of "wobbling motion" in the resonances, or in the reaction mechanism.

To review the formulation of the molecular model[13], section 2 is devoted. We discuss the coordinate system and the model hamiltonian in the rotating molecular frame. In order to solve couplings among molecular configurations, we

adopt a geometrical method instead of the coupled channel one. Simply speaking, with high spins interactions between oblate-deformed nuclei favor the alignment of their deformation axes, but the axes are mostly perpendicular to the reaction plane, i.e., the equator-equator configuration for oblate-oblate systems. To investigate dynamics of an interacting di-nuclear system around the configuration, we use the Euler angles of the deformed nuclei as dynamical variables rather than integrate them to obtain coupled-channel equations. In other words, they are internal collective variables of the rotating system. In order to formulate the model, we introduce a rotating molecular frame, z'-axis of which is parallel to the relative vector of two interacting nuclei. All the degrees of freedom of the system are transformed into the rotational motion of the total system and the internal motions referred to the rotating frame. And the dynamics of the latter degrees of freedom are treated as normal modes around the equilibrium.

In section 3, structures of the $^{28}\mathrm{Si} + {}^{28}\mathrm{Si}$ system are investigated. We firstly inspect the multi-dimensional energy surfaces and look for the equilibrium configurations of the system. In subsection 3.1., harmonic approximation is adopted to solve normal modes. An energy spectrum with good K-quantum number will be given. Subsection 3.2. is devoted for the analysis of the rotational motions(K-mixings) at extremely high spins. After K-mixing, the K-states are recombined into new states. Energy level sequences obtained by the diagonalizations of asymmetric rotators are given. In section 4, R-matrix theory and a method of angular correlations are briefly summarized. In section 5, results are presented and a comparison with experiments will be done. Summary is given in section 6.

§2. Reminder for Di-nuclear Structure of ^{28}Si $+^{28}$Si System

First, we briefly explain our molecular model for heavy-ion resonances. Definitions or derivations of the expressions are given in details, in Ref. 13(hereafter referred as Ref. I). We consider interacting two deformed nuclei such as $^{28}\mathrm{Si}+{}^{28}\mathrm{Si}$, and then the degrees of freedom are their relative motions and the orientations of the deformation axes of two nuclei. The latter degrees of freedom or configurations are usually treated as "channels" in the weak coupling picture, but we do not start from the motions of pure rotational states. We expect stable geometrical configurations with some confinements for those orientations. Really as mentioned later, each typical stable configuration appeared by rather strong

attractive nucleus-nucleus interaction between tips of two deformed nuclei, for prolate and oblate deformations, respectively. Then those orientations are important physical quantities which determine the geometrical configurations and furthermore should be regarded to be vibrational degrees of freedom around the equilibrium.

In order to describe the rotational motion of the whole system with a stable configuration, we define molecular axes, the z'-axes of which is taken to be parallel to the relative vector $R = (R, \theta_2, \theta_1)$, between the constituent nuclei. The orientations of the deformed constituent nuclei are given by the intrinsic axes of the nuclei and are described by the Euler angles (α_i, β_i), referring to the molecular axes. Assuming a constant deformation and axial symmetry of the constituent nuclei, for simplicity, we have seven degrees of freedom

$$(q_i) = (\theta_1, \theta_2, \theta_3, R, \alpha, \beta_1, \beta_2), \tag{2.1}$$

as illustrated in Fig. 3, where the Euler angles α_1 and α_2 are combined into new variables $\theta_3 = (\alpha_1 + \alpha_2)/2$ and $\alpha = (\alpha_1 - \alpha_2)/2$.

First we look the kinetic energy operator in terms of the above coordinates. The classical kinetic energy of the system can be given in terms of the energies associated with the relative motion (radial motion and rotational motion of two-ion centers) and the rotational motions of two constituent nuclei.

$$T = \frac{1}{2}\mu\dot{R}^2 + \frac{1}{2}{}^t\vec{\omega}'\boldsymbol{I}_\mu(R)\vec{\omega}' + \frac{1}{2}{}^t\vec{\omega}_1\boldsymbol{I}_1\vec{\omega}_1 + \frac{1}{2}{}^t\vec{\omega}_2\boldsymbol{I}_2\vec{\omega}_2, \tag{2.2}$$

where $\boldsymbol{R}$ denotes the relative vector between two nuclei, μ being the reduced mass $m_1m_2/(m_1+m_2)$ of two constituent nuclei with masses m_1 and m_2, and the c.m. energy of the total system is omitted. The second term of the r.h.s of Eq. (2.2) is the rotational energy of two constituent nuclei given by the angular velocity of the molecular frame $\vec{\omega}'$ and the moment of inertia tensor $\boldsymbol{I}_\mu(R)$. The diagonal components I_{11} and I_{22} of the inertia tensor are μR^2, the others being zero, which is associated with masses m_1 and m_2 at the relative distance R. Then the expression of the rotational energy is equal to usual one, $\frac{1}{2}\mu R^2(\dot{\theta}_2^2 + \dot{\theta}_1^2\sin^2\theta_2)$. The vectors $\vec{\omega}_1$ and $\vec{\omega}_2$ denote the angular velocities of the rotational motions of the constituent nuclei, ${}^t\vec{\omega}_i$ being the transpose of $\vec{\omega}_i$. The inertia tensors of two nuclei $\boldsymbol{I}_1$ and $\boldsymbol{I}_2$ are defined in the coordinate frames of their principal axes, *i.e.*, they are diagonal, whose diagonal elements are determined by the excitation energies of the members of the ground rotational bands of the constituent nuclei.

At this stage the angular velocities of the constituent nuclei $\vec{\omega}_i$'s in Eq. (2.2) are still those referred to the laboratory frame, so we have to express them in the molecular coordinate system, *i.e.*, in terms of the angular velocity of the molecular frame $\vec{\omega}'$ and those $\vec{\omega}_i''$ referred to the molecular frame. Then we express the total kinetic energy as a sum of three parts, the total rotational energy $T_{\rm rot}$ associated with $\vec{\omega}'$, the internal kinetic energy $T_{\rm int}$ and the Coriolis coupling term $T_{\rm C}$, as follows;

$$T = T_{\rm rot} + T_{\rm int} + T_{\rm C}, \tag{2.3}$$

$$T_{\rm rot} = \frac{1}{2} {}^t\vec{\omega}' \boldsymbol{I}_{\rm s} \vec{\omega}', \tag{2.4}$$

$$T_{\rm int} = \frac{1}{2}\mu\dot{R}^2 + \frac{1}{2} {}^t\vec{\omega}_1'' \boldsymbol{I}_1 \vec{\omega}_1'' + \frac{1}{2} {}^t\vec{\omega}_2'' \boldsymbol{I}_2 \vec{\omega}_2'', \tag{2.5}$$

$$T_{\rm C} = {}^t\vec{\omega}' \left\{ {}^tR'(\alpha_1\beta_1\gamma_1)\, \boldsymbol{I}_1 \vec{\omega}_1'' + {}^tR'(\alpha_2\beta_2\gamma_2)\, \boldsymbol{I}_2 \vec{\omega}_2'' \right\}, \tag{2.6}$$

where $R'(\alpha_i\beta_i\gamma_i)$ denotes the transformation matrix which connects the axes of the molecular frame and the principal axes of each constituent nucleus, The total rotational energy $T_{\rm rot}$ is the rotational energy of the interacting constituent nuclei as a whole system, which rotates with the angular velocity $\vec{\omega}'$. The inertia tensor is given by

$$\boldsymbol{I}_{\rm s} = \boldsymbol{I}_\mu(R) + {}^tR'(\alpha_1\beta_1\gamma_1)\, \boldsymbol{I}_1 R'(\alpha_1\beta_1\gamma_1) + {}^tR'(\alpha_2\beta_2\gamma_2)\, \boldsymbol{I}_2 R'(\alpha_2\beta_2\gamma_2), \tag{2.7}$$

where the first term of the r.h.s. denotes the moments of inertia of simple two-ion centers, and the second and third terms are contributions from the constituent nuclei individually, though their "rotations" are already taken into account in Eq. (2.5). The internal kinetic energy $T_{\rm int}$ is those associated with the orientation degrees of freedom of the constituent nuclei in addition to the radial motion between them. The last two terms of the r.h.s. of Eq. (2.5) have a form of rotational energy, but their motions are not necessarily rotational. This is why the quotations are put on the word rotations above. Actually the nucleus-nucleus interaction favors cohesion of two constituent nuclei. Motions in the orientations are, therefore, not necessary to be rotational but would be rather confined, such as a sticking of the constituent nuclei. In the sticking limit the angular velocities

$\vec{\omega}_i''$ are zero, while they are constant in free rotations. We, of course, anticipate intermediate stages between the sticking limit and the rotation, *i.e.*, fluctuations around the sticking configuration. For vibrational motions, for example, we consider fluctuations of the values of $\vec{\omega}_i''$ around zero, average values of them being to be zero.

After expressing those angular velocities with time derivatives of the corresponding Euler angles, we obtain a classical kinetic energy expression $\frac{1}{2}\sum g_{ij}\dot{q}_i\dot{q}_j$. And then we quantize it by using general formula for the curve-linear coordinate system. As the classical kinetic energy consists of the three parts, *i.e.* the total rotation, the internal motions and their couplings, the quantum mechanical kinetic energy $\hat{T}$ will be also divided into three terms as $\hat{T} = \hat{T}_{\rm rot} + \hat{T}_{\rm int} + \hat{T}_{\rm C}$. Naturally the term $\hat{T}_{\rm rot}$ is associated with the rotational variables $(\theta_1, \theta_2, \theta_3)$, $\hat{T}_{\rm int}$ with the internal variables $(R, \alpha, \beta_1, \beta_2)$ and $\hat{T}_{\rm C}$ with both. According to the derivation, $\hat{T}_{\rm rot}$ is expressed by the partial differential operators of the Euler angles of the molecular frame θ_i. We combined those differential operators into angular momentum operators $\hat{J}_i'$ referred to the molecular axes, as usual, *i.e.*,

$$\hat{T}_{\rm rot} = \frac{\hbar^2}{2} \sum_{\substack{1\le i\le 3 \\ 1\le j\le 3}} \mu_{ij}\hat{J}_i'\hat{J}_j'. \tag{2.8}$$

The coefficients μ_{ij} are given as follows, in terms of the internal variables $(R, \alpha, \beta_1, \beta_2)$.

$$\begin{aligned}
\mu_{11} &= \mu_{22} = \frac{1}{\mu R^2}, \\
\mu_{12} &= 0, \\
\mu_{13} &= \frac{1}{2\mu R^2}\cos\alpha(\cot\beta_1 + \cot\beta_2), \\
\mu_{23} &= \frac{1}{2\mu R^2}\sin\alpha(\cot\beta_1 - \cot\beta_2), \\
\mu_{33} &= \frac{1}{4}\Big[\Big(\frac{1}{I_1} + \frac{1}{\mu R^2}\Big)\frac{1}{\sin^2\beta_1} + \Big(\frac{1}{I_2} + \frac{1}{\mu R^2}\Big)\frac{1}{\sin^2\beta_2}\Big] - \frac{1}{2\mu R^2} \\
&\qquad + \frac{1}{2\mu R^2}\cos 2\alpha\cot\beta_1\cot\beta_2,
\end{aligned} \tag{2.9}$$

where I_1 and I_2 are the diagonal elements of the inertia tensors $\boldsymbol{I}_1$ and $\boldsymbol{I}_2$, respectively.

The internal kinetic energy operator is associated with the variables $(R, \alpha, \beta_1, \beta_2)$. as already mentioned. As usual, we introduce a volume element $dV = dR d\alpha d\beta_1 d\beta_2$

instead of the original $dV = DdRd\alpha d\beta_1 d\beta_2$ with $D = \mu^{3/2}R^2 I_1 \sin\beta_1 I_2 \sin\beta_2$, which means that the wave functions are defined with the additional factor $\sqrt{D}$. Accordingly we obtain

$$\hat{T}_{\rm int} = \hat{O}_{\rm int} + V_{\rm add}, \tag{2.10}$$

$$\begin{aligned}\hat{O}_{\rm int} = -\frac{\hbar^2}{2}\Bigg[&\frac{1}{\mu}\frac{\partial^2}{\partial R^2} + \Big(\frac{1}{I_1}+\frac{1}{\mu R^2}\Big)\frac{\partial^2}{\partial\beta_1^2} + \Big(\frac{1}{I_2}+\frac{1}{\mu R^2}\Big)\frac{\partial^2}{\partial\beta_2^2} + \frac{2\cos 2\alpha}{\mu R^2}\frac{\partial^2}{\partial\beta_1\partial\beta_2}\\ &+\frac{1}{4}\Bigg\{\Big(\frac{1}{I_1}+\frac{1}{\mu R^2}\Big)\frac{1}{\sin^2\beta_1} + \Big(\frac{1}{I_2}+\frac{1}{\mu R^2}\Big)\frac{1}{\sin^2\beta_2} - \frac{2}{\mu R^2}\Bigg\}\frac{\partial^2}{\partial\alpha^2}\\ &-\frac{\partial}{\partial\alpha}\frac{\cos 2\alpha}{2\mu R^2}\cot\beta_1\cot\beta_2\frac{\partial}{\partial\alpha}\\ &-\frac{1}{2\mu R^2}\Big(\cot\beta_2\frac{\partial}{\partial\beta_1}+\cot\beta_1\frac{\partial}{\partial\beta_2}\Big)\Big(\sin 2\alpha\frac{\partial}{\partial\alpha}+\frac{\partial}{\partial\alpha}\sin 2\alpha\Big)\Bigg],\end{aligned} \tag{2.11}$$

$$\begin{aligned}V_{\rm add} = -\frac{\hbar^2}{8}\Bigg[&\Big(\frac{1}{I_1}+\frac{1}{\mu R^2}\Big)\Big(\frac{1}{\sin^2\beta_1}+1\Big) + \Big(\frac{1}{I_2}+\frac{1}{\mu R^2}\Big)\Big(\frac{1}{\sin^2\beta_2}+1\Big)\\ &+\frac{2\cos 2\alpha}{\mu R^2}\cot\beta_1\cot\beta_2\Bigg],\end{aligned} \tag{2.12}$$

where $V_{\rm add}$ is the term so-called additional potential due to the new volume element.

The Coriolis coupling operator $\hat{T}_{\rm C}$ consists of coupling operators between the variables $(\theta_1,\theta_2,\theta_3)$ and $(R,\alpha,\beta_1,\beta_2)$, i.e.,

$$\begin{aligned}\hat{T}_{\rm C} = \frac{\hbar^2}{\mu R^2}\Bigg[&i\sin\alpha\Big(-\frac{\partial}{\partial\beta_1}+\frac{\partial}{\partial\beta_2}\Big)\hat{J}_1' + \cos\alpha\Big(\frac{\partial}{\partial\beta_1}+\frac{\partial}{\partial\beta_2}\Big)\,i\hat{J}_2'\\ &+\frac{i}{2}\sin 2\alpha\Big(-\cot\beta_2\frac{\partial}{\partial\beta_1}+\cot\beta_1\frac{\partial}{\partial\beta_2}\Big)\hat{J}_3'\\ &-\frac{i}{4}(\cot\beta_1-\cot\beta_2)\Big(\frac{\partial}{\partial\alpha}\cos\alpha\hat{J}_1' + \hat{J}_1'\cos\alpha\frac{\partial}{\partial\alpha}\Big)\\ &-\frac{i}{4}(\cot\beta_1+\cot\beta_2)\Big(\frac{\partial}{\partial\alpha}\sin\alpha\hat{J}_2' + \hat{J}_2'\sin\alpha\frac{\partial}{\partial\alpha}\Big)\Bigg]\\ +\frac{\hbar^2}{4}&\Big[\Big(\frac{1}{I_1}+\frac{1}{\mu R^2}\Big)\frac{1}{\sin^2\beta_1} - \Big(\frac{1}{I_2}+\frac{1}{\mu R^2}\Big)\frac{1}{\sin^2\beta_2}\Big]\Big(-i\frac{\partial}{\partial\alpha}\Big)\hat{J}_3',\end{aligned} \tag{2.13}$$

where the derivative operators of θ_i's are again rewritten with the angular momentum operators $\hat{J}'_i$.

For details of some relations and explicit expressions, see Appendices of Ref. I), for example, for the angular velocities in the molecular frame, the classical kinetic energy in terms of time derivatives of the Euler angles, their quantization and symmetries of the system.

In order to make the problem to be tractable, we start with good K-quantum number, which is expected to be appropriate for the system of small axial asymmetry. It would be discussed later in details whether the hypothesis is correct or not. For the $^{24}\mathrm{Mg} + {}^{24}\mathrm{Mg}$ system(prolate-prolate one), for example, it would be rather simple to intuitively understand it, because stable configurations at high spins are dominantly elongated pole-pole ones which keep axial symmetry. The $^{28}\mathrm{Si} + {}^{28}\mathrm{Si}$ system(oblate-oblate one), however, favors equator-equator configurations, the symmetry of which is more complicated. So we should return back to this problem, but anyhow at first we put K to be good. Actually the K-mixing terms in $\hat{T}_{\mathrm{rot}}$ with the coefficients μ_{13} and μ_{23} are relatively small, because they have the factor $1/\mu R^2$ which is much smaller than $1/I_i$ in the contact region. We, therefore, regroup the kinetic energy operator as follows,

$$\hat{T} = \hat{T}' + \hat{T}'_{\mathrm{C}}, \tag{2.14}$$

$$\hat{T}' = \hat{T}'_{\mathrm{rot}} + \hat{T}_{\mathrm{int}}, \tag{2.15}$$

where $\hat{T}'_{\mathrm{C}}$ includes the Coriolis coupling $\hat{T}_{\mathrm{C}}$ and the K-mixing terms in $\hat{T}_{\mathrm{rot}}$. Accordingly the new rotational operator $\hat{T}'_{\mathrm{rot}}$ has good K-quantum number. Hereafter firstly we restrict our discussion to *the rotation and vibration operator* $\hat{T}'$, together with the interaction potential given later. Then the axial asymmetry of the system in the ground and excited states would be explored. And next, the effects of K-mixing due to the operator $\hat{T}'_{\mathrm{C}}$, i.e., the Coriolis coupling terms etc. will be discussed.

As our kinetic energy operator $\hat{T}'$ keeps good K-quantum number, eigenstates of the system are of a rotation-vibration type,

$$\Psi_\lambda \sim D^J_{MK}(\theta_i)\chi_K(R, \alpha, \beta_1, \beta_2). \tag{2.16}$$

Now the problem to be solved is internal motions, i.e., motions associated with the internal variables $(R, \alpha, \beta_1, \beta_2)$ which couple with each other through the kinetic

energy operator $\hat{T}'$ and the interaction potential. For the later use in section 3, we define centrifugal potential given by $\hat{T}'_{\rm rot}$ with specified J and K,

$$T_{\rm rot}(J,K) = \frac{\hbar^2}{2}\Bigg[\frac{1}{\mu R^2}\Big\{J(J+1) - \frac{3}{2}K^2 + \frac{1}{2}\cos 2\alpha \cot\beta_1 \cot\beta_2 (K^2-1)\Big\} + \Big(\frac{1}{I}+\frac{1}{\mu R^2}\Big)\Big(\frac{K^2-1}{4\sin^2\beta_1} + \frac{K^2-1}{4\sin^2\beta_2} - \frac{1}{2}\Big)\Bigg], \tag{2.17}$$

where I denotes the moment of inertia of the constituent nuclei, i.e., $I = I_1 = I_2$, since we are interested in the symmetric system. In the expression of $T_{\rm rot}(J,K)$, we use the eigenvalue K instead of $\hat{J}'_3$. Note that the additional potential $V_{\rm add}$ of Eq. (2.12) in $\hat{T}_{\rm int}$ is moved into $T_{\rm rot}(J,K)$ for convenience, and similar terms in $\hat{T}$ and $V_{\rm add}$ are amalgamated.

For the interaction potential we want to have such one which depends on geometrical configurations of interacting nuclei, i.e., potential as a function of the Euler angles of the nuclei in addition to the radial distance between them. Proximity potentialappears to be one of the most suitable potentials[20], but it is fairly laborious to calculate it for various configurations, i.e., one has to find out the shortest distance between two curved surfaces of arbitrarily oriented deformed nuclei and to calculate curvatures etc. at the point. Instead, we employ the folding method. Since, in the double folding model, nuclear densities corresponding to geometrical molecular configurations are directly folded with effective nucleon-nucleon interactions, the model easily provides an interaction potential for the present purpose, i.e., as a function of the collective variables. We use the following nucleon-nucleon interaction, called *density dependent* M3Y(DDM3Y)[21],

$$v(E,\rho,r) = f(E,\rho)g(E,r), \tag{2.18}$$

where $f(E,\rho)$ gives nucleon-density dependence by

$$f(E,\rho) = C(E)[1+\alpha(E)e^{-\beta(E)\rho}], \tag{2.19}$$

ρ denoting density of nuclear matter in which the interacting nucleons are embedded, and $g(E,r)$ describes original nucleon-nucleon interaction,

$$g(E,r) = \left[7999\frac{{\rm e}^{-4r}}{4r} - 2134\frac{{\rm e}^{-2.5r}}{2.5r}\right] + \hat{J}(E)\delta(\boldsymbol{r}). \tag{2.20}$$

The first term of $g(E,r)$ is M3Y potential without OPEP and the second term represents single-nucleon exchange suggested by Satchler and Love[22]. E is the bombarding energy per nucleon, which we choose as suitable for the resonance energies($E = 3.75$MeV corresponding to $E_{Lab.} = 105$ MeV for $^{28}\mathrm{Si} + ^{28}\mathrm{Si}$). At a short distance of the folding potential, i.e., with highly overlapping densities, DDM3Y gives slightly weak attractive potential. At the normal density, for example, the density-dependent factor $f(E,\rho)$ reduces about 75% of the interaction strength compared with the original $g(E,r)$, while it enhances about 20% at the half density, i.e., at the contact region.

The folding-model potential, however, is considered to be accurate only in the tail region of the nucleus-nucleus interaction. In the region of nuclear-density overlap going beyond the normal density, its accuracy is doubtful. Hence, in addition to folding the nucleon-nucleon interaction, we introduce a phenomenological repulsive potential which would originate from the effects of the Pauli principle among nucleons belonging to the interacting nuclei respectively or from the compression effects due to overlapping density. We estimate the strength of the repulsive potential due to compression of nuclear density, from the equation of state of nuclear matter, i.e., from binding energy as a function of nuclear density. One may think that the picture of the density overlap is doubtful in low energy, but the folding model does not take into account density redistribution, so it is consistent to account higher densities in overlapping region. Anyhow, what we are interested in is dynamics of two interacting nuclei in high spins which are dominated by strong centrifugal forces. Therefore the long-range part of interactions is crucially important, not the short-range part, which is treated more or less in a phenomenological way.

The folding potential is defined as usual,

$$\begin{aligned} U(\boldsymbol{R}) &= \int d\boldsymbol{r}_1 \int d\boldsymbol{r}_2\, \rho_1(\boldsymbol{r}_1)\rho_2(\boldsymbol{r}_2)v(\boldsymbol{r}_{12}), \\ \boldsymbol{r}_{12} &= \boldsymbol{R} + \boldsymbol{r}_2 - \boldsymbol{r}_1, \end{aligned} \tag{2.21}$$

where $\boldsymbol{R}$ is the relative vector between the interacting nuclei and $\boldsymbol{r}_i$ are referred to the centers of the nuclei respectively. The long-range attractive part of the interaction potential in the molecular frame V_{attr} is obtained from $U(\boldsymbol{R})$ by taking the vector $\boldsymbol{R}$ to be parallel to the z'-axis and by fixing orientations of the density distributions of the constituent nuclei to the molecular frame. By using Fourier

transformation,

$$V_{\rm attr} = \frac{1}{2\pi^2}\sum_{lm} i^{-l} Y_{lm}(\hat{\boldsymbol{R}}) \int dk k^2 j_l(kR) \int d\hat{k} Y^*_{lm}(\hat{\boldsymbol{k}}) \tilde{v}(\boldsymbol{k}) \tilde{\rho}_1(\boldsymbol{k}) \tilde{\rho}_2(-\boldsymbol{k}), \tag{2.22}$$

$$\tilde{v}(\boldsymbol{k}) = \int d\boldsymbol{r} e^{i\boldsymbol{k}\boldsymbol{r}} v(r) = 4\pi \int dr r^2 j_0(kr) v(r), \tag{2.23}$$

$$\tilde{\rho}_i(\boldsymbol{k}) = \int d\boldsymbol{r}' e^{i\boldsymbol{k}\boldsymbol{r}'} \rho_i(\boldsymbol{r}'). \tag{2.24}$$

The density distribution $\rho_i(\boldsymbol{r}')$ in the molecular frame is related to that in the body-fixed frame, i.e., to that in the principal axes of the constituent nucleus; by Euler rotations, $\rho_i(\boldsymbol{r}') = \hat{\mathcal{R}}(\alpha_i\beta_i\gamma_i)\rho_i^B(\boldsymbol{r}') = \rho_i^B(\boldsymbol{r}'')$, where $\rho_i^B(\boldsymbol{r}'')$ is the density distribution in the principal axes and therefore

$$\rho_i^B(\boldsymbol{r}'') = \sum_l \rho_l(r'') Y_{l0}(\hat{\boldsymbol{r}}'') \tag{2.25}$$

with the assumed axial symmetry of the constituent nucleus. So the Fourier transform $\tilde{\rho}_i(\boldsymbol{k})$ is given with the Euler angles included as parameters,

$$\tilde{\rho}_i(\boldsymbol{k}) = \sum_l i^l \tilde{\rho}_l(k) \sum_{m'} D^{l*}_{m'0}(\alpha_i\beta_i\gamma_i) Y_{lm'}(\hat{\boldsymbol{k}}), \tag{2.26}$$

$$\tilde{\rho}_l(k) = 4\pi \int dr r^2 j_l(kr) \rho_l(r). \tag{2.27}$$

Inserting Eq. (2.26) with $i = 1$ and 2 into Eq. (2.22), we obtain the final form of the interaction potential as a function of the internal variables $(R, \alpha, \beta_1, \beta_2)$ as in the following,

$$V_{\rm attr}(R,\alpha,\beta_1,\beta_2) = \sum_{l'l''l} (2\pi)^{-3} i^{l'-l''-l} \hat{l}'\hat{l}''(l'l''00 \mid l0) \times F_{l'l''l}(R) G_{l'l''l}(\alpha,\beta_1,\beta_2), \tag{2.28}$$

$$F_{l'l''l}(R) = \int dk k^2 j_l(kR) \tilde{v}(k) \tilde{\rho}_{l'}(k) \tilde{\rho}_{l''}(k), \tag{2.29}$$

$$G_{l'l''l}(\alpha,\beta_1,\beta_2) = \sum_{m\geq 0} (-1)^m (2-\delta_{m0})(l'l''m-m \mid l0) \times \cos(2m\alpha) d^{l'}_{m0}(\beta_1) d^{l''}_{m0}(\beta_2). \tag{2.30}$$

It should be mentioned here that γ_i does not appear in the final expression due to the D-function with one magnetic quantum number being zero which originates from the axially symmetric density distribution in Eq. (2.25), and that α_1 and α_2 are combined into $2\alpha = \alpha_1 - \alpha_2$ due to the fact that the vector $\boldsymbol{R}$ is parallel to z'-axis, i.e., the magnetic quantum number associated with $\boldsymbol{R}$ is zero. The Coulomb interaction is also folded, together with nuclear interaction $v(E, \rho, r)$ of Eq. (2.18).

We assume a density profile of $\rho_i^B(\boldsymbol{r}'')$ to be the Fermi distribution with $\rho_i^B(\boldsymbol{r}'') = \rho_0/[1 + \exp\{(r'' - R_{\rm N}(\boldsymbol{r}''))/a_{\rm N}\}]$, $R_{\rm N}(\boldsymbol{r}'')$ denoting the radius of the deformed nucleus. As for the deformation of the constituent ^{28}Si nuclei, the existence of hexadecapole deformation ($\beta_4 = 0.20 \pm 0.03$) is suggested from coupled-channel analyses for elastic and inelastic neutron scattering[23]. Therefore we take the radius of each nucleus as $R_{\rm N}(\boldsymbol{r}'') = r_0 A_i^{1/3}[1 + \beta_{\rm Q} Y_{20}(\hat{\boldsymbol{r}}'') + \beta_{\rm H} Y_{40}(\hat{\boldsymbol{r}}'')]$ including two parameters $\beta_{\rm Q}$ and $\beta_{\rm H}$ for deformation, the values of which are determined to be -0.46 and 0.22, respectively, according to the suggested value for ratio $\beta_{\rm Q}/\beta_{\rm H}$ and their magnitudes adjusted with $B(E2)$ value of the ground-rotational band of ^{28}Si[24]. The value of r_0 is taken to be 1.03fm from the textbook of Bohr-Mottelson[25], and $a_{\rm N}$ to be 0.48fm to reproduce RMS radius of the ground state.

Next, we proceed to the effect of density overlap in the inner region, where the folding potential is not expected to be adequate. An overlapping of the densities brings about a higher nuclear density than normal one, which gives rise to a binding energy loss of the interacting system additionally to the attractive folding potential. We take into account the effect as a repulsive potential to be added to the folding one given in Eq. (2.21). A volume with the higher density depends on configurations of the constituent nuclei, especially on their relative distance. Actually, overlappings of two nuclei produce nuclear densities from zero to twice of the normal density. An accurate calculation of the effect, therefore, is fairly laborious. We propose a simple approximate way. If we assume the density profile to be of sharp cut-off or with a very small diffuseness, an overlapping volume has always twice of the normal density. So the short-range repulsive potential is expected to be proportional to the overlapping volume,

$$V_{\rm rep}(R, \alpha, \beta_1, \beta_2) = V_{\rm P} \int \delta(\boldsymbol{r}_{12}) \rho_1'(\boldsymbol{r}_1) \rho_2'(\boldsymbol{r}_2) d\boldsymbol{r}_1 d\boldsymbol{r}_2, \qquad (2.31)$$

where the primes on the densities indicate Fermi distribution with a small dif-

fuseness. The strength V_P is chosen in the following, referring the Equation of State(EOS) of nuclear matter. This looks like a folding potential of the zero-range interaction, but has the primed densities instead of the normal density distributions. Of course we can utilize a merit of the form of Eq. (2.31) in actual calculations.

As a reference we can simulate the proximity potential for some simple configurations, with an interaction potential $V_{\rm int}$ in the above formula, i.e.,

$$V_{\rm int} = V_{\rm attr} + V_{\rm rep}, \tag{2.32}$$

by adjusting the diffuseness a_P in ρ' and the strength V_P freely. Those simulations were successfully done as a test of $V_{\rm int}$, i.e., we reproduced the radial dependence of the proximity potential for $R > 4$fm for the *pole-pole configurations* of the ^{24}Mg + ^{24}Mg system, by adjusting the repulsive potential(see Ref.I). It was, however, found that the proximity potential is effectively much weaker than those potentials which have quasi-bound states, and not favorable concerning molecular resonance calculations.

As the other way to determine the strength V_P, we use EOS of the nuclear matter, i.e., a binding energy loss per nucleon $\Delta\varepsilon$ for twice of the normal density which is calculated under the condition of complete overlap at $R = 0$ limit. Without Coulomb energy the value of $\Delta\varepsilon$ can be taken to be $7 \sim 11$MeV[26] from the values of the nuclear compression modulus $K_\infty = 180 \sim 240$MeV[27], which is suggested by the experiments on giant monopole resonances. Hence the values $a_P = 0.25$fm and $V_P = 330$MeVfm^3 are obtained to reproduce $\Delta\varepsilon = 9$MeV in ^{28}Si + ^{28}Si system. Radial forms of the folding potential are shown in Fig. 4, where the interaction potential (indication J=0-Y2+Y4) and the effective potential for $J = 38$ (solid line) are displayed for the stable geometrical configurations (parallel equator-equator ones, see the next section).

§3. Di-nuclear structures of ^{28}Si + ^{28}Si

3.1. Harmonic approximation and normal modes with specified K

In order to know dynamical aspects of multi-dimensional internal motion, we calculate an effective potential with specified spin J and K, defined as follows:

$$V_{JK}(R, \alpha, \beta_1, \beta_2) = V_{\rm int}(R, \alpha, \beta_1, \beta_2) + T'_{\rm rot}(J, K). \tag{3.1}$$

In Fig. 5, an $R-\beta(\beta_1=\beta_2)$ energy surface, i.e., $V_{JK}(R,\pi/2,\beta,\beta)$ is displayed for $J=38$ and $K=0$. We find a local minimum point at $\beta_1=\beta_2=\pi/2$ and $R=7.6$fm, namely, at the equator-equator(E-E) configuration, with a rather deep potential well around the equilibrium. In Fig. 6(a), α-dependence of V_{JK} in the E-E configuration at the equilibrium distance is shown. (Note that our definition of the domain of the variables are $0\leq\alpha<\pi$ and $0\leq\beta_1,\beta_2\leq\pi$.) We find the α-dependence is extremely weak. Another point is that we have two local minima at $\alpha=0$ and $\pi/2$. Those two configurations are, however, exactly the same, namely, *parallel* E-E configuration (z''-axes of the constituent nuclei are parallel). Therefore it is necessary to impose symmetrization on the wave functions. In Fig. 6(b), β-dependences of V_{JK} with $\beta_1=\beta_2$ are compared between at $\alpha=0$ and at $\alpha=\pi/2$, where solid line is for $\alpha=\pi/2$ (the cross section of Fig. 5 at $R=R_{\rm e}=7.6$fm) and dashed line for $\alpha=0$. (Note that configurations with $\beta_1=\beta_2\neq\pi/2$ at $\alpha=0$ are not the same as those with the same β_i-values at $\alpha=\pi/2$, but are the same as those with $\beta_1=\pi-\beta_2$ at $\alpha=\pi/2$.) The β-well at $\alpha=\pi/2$ is seen to be rather shallow, compared with that at $\alpha=0$. Hence, in addition to the weak α-dependence of V_{JK} in the E-E configuration, we have significantly α-dependent restoring force for β-motions around the E-E configuration.

In order to solve normal modes for four variables $(R,\alpha,\beta_1,\beta_2)$, we expand V_{JK} into a quadratic form for R, β_1 and β_2, at the equilibrium E-E configuration, while for α we keep its dependence exactly in a form of $\cos(2m\alpha)$ series, such as those given in the interaction potential of Eq. (2.30). Then the effective potential is expressed as

$$\begin{aligned} V_{JK}(R,\alpha,\beta_1,\beta_2) =& V_{JK}(R_{\rm e},\alpha,\frac{\pi}{2},\frac{\pi}{2})+\frac{k_R}{2}(R-R_{\rm e})^2 \\ &+\frac{1}{2}k_\beta^{11}(\alpha)\Delta\beta_1^2+\frac{1}{2}k_\beta^{22}(\alpha)\Delta\beta_2^2 \\ &+k_\beta^{12}(\alpha)\Delta\beta_1\Delta\beta_2+(\textit{higher order}), \end{aligned} \tag{3.2}$$

where $\Delta\beta_i$ denotes $\beta_i-\pi/2$. $k_\beta^{ij}(\alpha)$ denotes the second derivative $\partial^2V_{JK}/\partial\beta_i\partial\beta_j$, $k_\beta^{11}(\alpha)$ being equal to $k_\beta^{22}(\alpha)$. Although $k_\beta^{ij}(\alpha)$ is a coefficient of $\Delta\beta_i\Delta\beta_j$ in the expansion, it is a function of α, i.e., we take into account α-dependence of the coefficient, in addition to the α-dependence of $V_{JK}(R_{\rm e},\alpha,\frac{\pi}{2},\frac{\pi}{2})$. As $k_\beta^{11}(\alpha)$ consists of $\cos(2m\alpha)$ series with $m=$ *even* including zero, the major part is a

constant k_0 from $m = 0$. We write $k_\beta^{11}(\alpha) = k_\beta^{22}(\alpha) = k_0 + k_2(\alpha)$, $k_2(\alpha)$ being a sum of contributions from terms with $m = even > 0$.

We introduce new coordinates in order to eliminate cross products of β_1 and β_2 both in $T_{\rm int}$ and in the quadratic expansion of V_{JK}. The new variables are *butterfly* and *anti-butterfly* as follows:

$$\begin{aligned} \beta_+ &= (\Delta\beta_1 + \Delta\beta_2)/\sqrt{2} = (\beta_1 + \beta_2 - \pi)/\sqrt{2}, \\ \beta_- &= (\Delta\beta_1 - \Delta\beta_2)/\sqrt{2} = (\beta_1 - \beta_2)/\sqrt{2}. \end{aligned} \tag{3.3}$$

Furthermore the inertia masses of three variables α, β_+ and β_- are approximated by the values given at E-E configuration. Combining the kinetic energy operator and expanded effective potential, the total hamiltonian is given as follows:

$$H = H_0 + T_{\rm C}' + (higher\ order), \tag{3.4}$$

$$H_0 = H_R + H_{\rm angl}(\beta_+, \beta_-, \alpha), \tag{3.5}$$

$$H_R = -\frac{\hbar^2}{2\mu}\frac{\partial^2}{\partial R^2} + \frac{k_R}{2}(R - R_{\rm e})^2, \tag{3.6}$$

$$\begin{aligned} H_{\rm angl}(\beta_+, \beta_-, \alpha) = {} & H_+(\beta_+, \alpha) + H_-(\beta_-, \alpha) \\ & - \frac{\hbar^2}{4I}\frac{\partial^2}{\partial\alpha^2} + V_{JK}(R_{\rm e}, \alpha, \frac{\pi}{2}, \frac{\pi}{2}), \end{aligned} \tag{3.7}$$

$$H_\pm(\beta_\pm, \alpha) = -\frac{\hbar^2}{2}\left(\frac{1}{I} + \frac{1 \pm \cos 2\alpha}{\mu R_{\rm e}^2}\right)\frac{\partial^2}{\partial\beta_\pm^2} + \frac{k_\pm(\alpha)}{2}\beta_\pm^2, \tag{3.8}$$

where $+$ or $-$ sign of $\pm$ in Eq. (3.8) corresponds to β_+ and β_- degrees of freedom, respectively, with $k_+(\alpha) = k_0 + k_2(\alpha) + k_\beta^{12}(\alpha)$ and $k_-(\alpha) = k_0 + k_2(\alpha) - k_\beta^{12}(\alpha)$.

Now we solve the Schrödinger equation with the hamiltonian H_0 for the internal four degrees of freedom, which is separated into two parts. One is a hamiltonian H_R for radial motion and nothing but that of a simple one dimensional harmonic oscillator. Another is $H_{\rm angl}$ for the angle variables α, β_+ and β_-, which is also *almost separable* into H_+ of β_+, H_- of β_- and remaining hamiltonian for α. H_+ and H_- again represent harmonic oscillators, although the masses and the restoring forces depend on α. Hence we analytically obtain wave functions for $H_\pm$ and their energy quanta $\hbar\omega_\pm$ with the frequencies

$$\omega_\pm = \sqrt{k_\pm(\alpha)\left(\frac{1}{I} + \frac{1 \pm \cos 2\alpha}{\mu R_{\rm e}^2}\right)}\ . \tag{3.9}$$

Taking into account those vibrational energies from β-degrees of freedom, we introduce a reduced potential for α-motion, and obtain a Schrödinger equation for α-motion as follows:

$$\left[-\frac{\hbar^2}{4I}\frac{\partial^2}{\partial\alpha^2} + V_{JK}(R_e, \alpha, \frac{\pi}{2}, \frac{\pi}{2}) + E^{\beta}_{n_+,n_-}(\alpha) \right]\phi(\alpha) = E_{\rm angl}\phi(\alpha), \qquad (3.10)$$

where $E^{\beta}_{n_+,n_-}(\alpha)$ denotes vibrational energy $(n_+ + 1/2)\hbar\omega_+ + (n_- + 1/2)\hbar\omega_-$ from $H_+ + H_-$, added as a part of the reduced potential. Note that, in order to obtain analytic form of $\hbar\omega_\pm$ in $\cos(2m\alpha)$ series, we expand square root in Eq. (3.9) supposing $\omega_0 = \sqrt{k_0(1/I + 1/\mu R_e^2)}$ to be the leading term. We do not know simple analytic solutions of Eq. (3.10). As the reduced potential $V_{JK}(R_e, \alpha, \frac{\pi}{2}, \frac{\pi}{2}) + E^{\beta}_{n_+,n_-}(\alpha)$ is described by a sum of $\cos(2m\alpha)$, we consider a solution $\phi(\alpha)$ described by cosine and sine functions of α, i.e., Fourier series. Then Eq. (3.10) is reduced to a secular equation, which is easily solved. Thus the eigenenergy of the system is given as follows, specified by the quantum numbers $(n, n_+, n_-, K, (\nu, \pi_\alpha))$,

$$\begin{aligned} E^J(n, n_+, n_-, K, (\nu, \pi_\alpha)) =& E_0(R_e) + \frac{\hbar^2}{2}\left[\frac{J(J+1) - K^2 - 1}{\mu R_e^2} + \frac{K^2 - 2}{2I}\right] \\ &+ \left(n + \frac{1}{2}\right)\hbar\omega_R \\ &+ (n_+ + n_- + 1)\hbar\omega_0 + E^{\alpha}_{\nu}(\pi_\alpha), \end{aligned} \qquad (3.11)$$

where ν denotes a dominant frequency of α-motion with π_α for a parity concerning a reflection in the equilibrium of $\alpha = \pi/2$. The first and second terms in r.h.s. of Eq. (3.11) are constant energies from the interaction potential and the centrifugal energy included in V_{JK} at the equilibrium, respectively. $(n_+ + n_- + 1)\hbar\omega_0$ and $E^{\alpha}_{\nu}(\pi_\alpha)$ are vibrational energies for β-motions without α-dependence and the energy for α-motion, respectively.

There is a selection rule $\nu = even$ for $K = even$ and $\nu = odd$ for $K = odd$ $(K \pm \nu = even)$, for α-motion. If n_+ is equal to n_-, then $K \pm \nu = 4m$, m being an integer. Because of the parity and boson symmetries, n_+ can be taken to be larger than or equal to n_-. For β-vibrational modes, we have a rule $(-1)^{n_+ + n_-} = (-1)^K$ due to symmetry of each constituent nucleus under space inversion. n_+ is also related to the parity of α-motion as $\pi_\alpha = (-1)^{n_+}$. As a special case for $K = 0$, both n_+ and n_- are even, i.e., π_α is positive, due to parity symmetry.

In Fig. 7, molecular normal modes of $^{28}Si + ^{28}Si$ with spin 38 is displayed, where a pair of quanta (n_+, n_-) is given below the levels. Also given at the upper right-hand-side of the levels is a dominant quantum number ν for α-motion, which means α-motion is approximately described by $\cos\nu\alpha$ (or $\sin\nu\alpha$). Apparently K-excitation and twisting rotational modes appear to be lower than β-vibrational modes. The excitation energy for $K = 2$ is very small, smaller than 1MeV, and even those for $K = 4$ or $\nu = 4$ are smaller than 3MeV. In Fig. 8(a), a few examples of wave functions for α-motion are shown, where $\nu = 0$, and β-modes are in zero-point oscillation or 2quanta excitation of butterfly. We see that, with zero quanta for β-modes, the amplitude is wriggling around the value of a unit, the equilibria $\alpha = 0$ and $\pi/2$ being slightly favored. (With exact $\nu = 0$ we have a constant behavior. Weak $\nu = 4$ mixing exists.) With 2quanta for the butterfly mode, however, we find surprisingly strong concentration around the equilibrium of $\alpha = \pi/2$. In Fig. 8(b), we inspect the reduced α-potential for quanta $(2,0)$. Compared with the potential for $(0,0)$, we find that the minimum at $\alpha = 0$ disappears, and the potential well at $\alpha = \pi/2$ is extended to wider region, which sustains the localization of the amplitude. One may wonder why the difference between $\alpha = 0$ and $\pi/2$ exists. The reason is as follows: at $\alpha = 0$, due to the definition of $\beta_\pm$, β-motion with $(n_+, n_-) = (2,0)$ does not imply butterfly excitation but anti-butterfly one with 2quanta. Such a characteristic of $\beta_\pm$ coordinates gives larger excitation energy for $(2,0)$ at $\alpha = 0$ than at $\alpha = \pi/2$. In Fig. 8(c), energy quanta $\hbar\omega_\pm$ is shown versus α, where we are able to confirm the point. Returning back to di-nuclear configuration, for a configuration with $\beta_1 = \beta_2 < \pi/2$, for example, we obtain a butterfly one at $\alpha = \pi/2$, such as displayed in Fig.7, while at $\alpha = 0$ we obtain an anti-butterfly one with the same values of β_i. Hence the localization around $\alpha = \pi/2$, seen in Fig. 8(a), indicates nothing but a realization of a physical butterfly excitation. Thus we are able to classify the levels in Fig. 7 into two groups, i.e., twisting mode and butterfly mode (or anti-butterfly), for which (t) or (b) mark is assigned at the bottom of the figure, respectively.

3.2 Rotational motion at extremely high spins

One of the characteristic feature of the spectrum is series of low-energy K-rotational excitation due to axial asymmetry around molecular z-axis, which is in contrast with $^{24}Mg + ^{24}Mg$ case.[12,13] One can understand the reason im-

mediately from Fig. 9, where the upper configuration(^{24}Mg + ^{24}Mg) has axial symmetry as a whole, but the lower one for ^{28}Si + ^{28}Si has axial asymmetry. Approximately a triaxial system rotates around the axis with the maximum moments of inertia. By the definition of the axes in the lower panel of Fig. 9, we have $I_x > I_y >> I_z$. Thus two pancakes-like objects(^{28}Si) touching side-by-side may rotate around x-axis which is normal to the reaction plane. In the following we investigate again rotational motions by means of asymmetric-rotator hamiltonian, which is written as follows;

$$\hat{T}_{\rm rot} = \frac{\hat{J}_x^2}{2I_x} + \frac{\hat{J}_y^2}{2I_y} + \frac{\hat{J}_z^2}{2I_z}, \tag{3.12}$$

$$= \frac{\hat{J}^2}{2I_{\rm av}} + \frac{1}{2\Delta}\left(- \hat{J}_x^2 + \hat{J}_y^2\right) + \frac{1}{2I_K}\hat{J}_z^2, \tag{3.13}$$

where $I_{\rm av}$, Δ and I_K are related to I_x, I_y and I_z by

$$\frac{1}{I_{\rm av}} = \frac{1}{2}\left(\frac{1}{I_x} + \frac{1}{I_y}\right), \tag{3.14}$$

$$\frac{1}{\Delta} = -\frac{1}{I_x} + \frac{1}{I_{\rm av}} = \frac{1}{I_y} - \frac{1}{I_{\rm av}}, \tag{3.15}$$

$$\frac{1}{I_K} = \frac{1}{I_z} - \frac{1}{I_{\rm av}}. \tag{3.16}$$

By using up and down operators of the angular momentum in the body-fixed frame, we obtain

$$\hat{T}_{\rm rot} = \frac{\hat{J}^2}{2I_{\rm av}} + \frac{\hat{J}_z^2}{2I_K} - \frac{1}{4\Delta}\left(\hat{J}_+^2 + \hat{J}_-^2\right), \tag{3.17}$$

where $\hat{J}'_\pm \equiv \hat{J}'_x \pm i\hat{J}'_y$ denote up-down operators which give rise to couplings between defferent K's. The coupling strength is given by the coefficient $\frac{1}{\Delta}$, which is proportional to the difference between $\frac{1}{I_y}$ and $\frac{1}{I_x}$. In an intuitive understanding, the rotation around x-axis is lower in energy than the rotation around y-axis due to $I_x > I_y$. When the energy difference between the rotations around the molecular x- and y-axes is larger than K-excitation energies, the K-mixing would be rather large, In other words, an energetically favored motion, i.e., rotation around x-axis would be realized by the K-mixing. And then the spin orientations of two ^{28}Si nuclei are on the plane in consistent with "m=0", because the nuclei rotate around the axes perpendicular to their symmetry ones.

In order to obtain an accurate description of this triaxial rotator, as it is well known for polyatomic molecules, we diagonalize the Hamiltonian with an asymmetric inertia tensor, which gives rise to a mixing of K-projections of the total spin J[28]. The resultant motion should be called as "wobbling mode"[29]. The energy spectrum is displayed in Fig. 10(b) compared with the spectrum without K-mixings in Fig. 10(a). Now the states of low lying K-series are not the eigenstates as themselves, but are recomposed into new states. It is much interesting that we again obtain several states including $K = 0$ components as a result of K-mixing, which we may observe in the scattering. Those states are closely located in energy and so in good agreement with several fine peaks observed in the experiment. It should be noted here that the treatment of the asymmetric hamiltonian is somehow phenomenological and we assumed the same parameter for the coupling strength Δ for the molecular ground-band states and for the butterfly states.

As an analytical prescription, in the high spin limit ($K/J \sim 0$), the diagonalization in the K-space is found to be equivalent to solving a differential equation of the harmonic oscillator with parameters given by the moments of inertia. Thereby, the solution is a gaussian, or a gaussian multiplied by an Hermite polynomial,

$$f_n(K) = H_n(\frac{K}{b}) \exp\left[-\frac{1}{2}\left(\frac{K}{b}\right)^2\right], \tag{3.18}$$

where the width b is given by

$$b = (2J^2 I_K/\Delta)^{1/4}. \tag{3.19}$$

In order to calculate angular correlations we use those analytic forms in Eq. (3.18), which is simple and easy way to understand extent of K-mixing. Of course we can utilize numerical values obtained in the diagonalization procedure, but the values are almost the same as those given by the analytic form. Due to the lowest state $f_0(K)$ of Eq. (3.18), we have the wave function for the wobbling ground state as

$$\Psi_\lambda^{JM} \sim \sum_K \exp(-K^2/2b^2) D^J_{MK}(\theta_i) \chi_K(R, \alpha, \beta_1, \beta_2), \tag{3.20}$$

where in general, χ_K can be any molecular excitation mode, such as the ground-state configuration (parallel equator-equator one), butterfly mode and twisting ($\nu = 4$) mode, for which we examine the angular correlations.

§4. Decay Properties and Angular Correlations

4.1 R-matrix formalism

The asymptotic scattering wave function in the "channel" c' is written in the form with collision matrix $U_{c'c}$ as

$$\psi_{c'} \sim (G_c - iF_c)\delta_{c'c} - U_{c'c}(G_{c'} + iF_{c'}), \tag{4.1}$$

where c' is considered to include also the channel spin I' and the orbital angular momentum l'. F_c and G_c denote regular and irregular Coulomb wave functions for c, i.e. for the channel c and l, respectively. By using R-matrix formula, we obtain

$$U_{c'c} = \frac{e^{-i\sigma_c}u_c^{(-)}}{e^{i\sigma_c}u_c^{(+)}}\delta_{c'c} - i\sum_{\lambda JM}\frac{u^J_{\lambda c'}\tilde{u}^{J*}_{\lambda c}}{N^J_\lambda(E - W^J_\lambda)}, \tag{4.2}$$

where $u_c^{(-)}$ and $u_c^{(+)}$ denote usual incoming and outgoing waves, respectively, such as

$$\begin{aligned} u_c^{(-)} &= e^{i\sigma_c}(G_c - F_c), \\ u_c^{(+)} &= e^{-i\sigma_c}(G_c + F_c), \end{aligned} \tag{4.3}$$

with σ_c being the Coulomb phase shift. In the second term of Eq. (2), W^J_λ is a resonance pole, i.e., $W^J_\lambda = E^J_\lambda - \frac{i}{2}\Gamma^J_\lambda$, and N^J corresponds to a factor for the normalization of the resonance state, which is close to unit. $u^J_{\lambda c}$'s are given by

$$u^J_{\lambda c} = \frac{\sqrt{2k_c a_c}}{e^{i\sigma_c}u_c^{(+)}}\gamma^J_{\lambda c}, \tag{4.4}$$

with the reduced widths $\gamma^J_{\lambda c}$ from the amplitudes of the resonance states in the channel c, which is obtained by

$$\gamma^J_{\lambda c} = \left(\frac{\hbar^2}{2\mu_c a_c}\right)^{1/2} a_c y_c(a_c) = \left(\frac{\hbar^2}{2\mu_c a_c}\right)^{1/2}\frac{1}{a_c}\int \mathcal{I}^{JM*}_{cIl}\Psi^{JM}_\lambda dS, \tag{4.5}$$

where $\mathcal{I}^{JM*}_{cIl}$ denote channel wave functions, and S being the surface with channel radii a_c. Definition of our collision matrix $U_{c'c}$ is almost the same as those of Lain-Thomas[18] , but is different in a phase factor from them,

$$U_{c'c}(\text{Lain} - \text{Thomas}) = e^{i(\sigma_{cl} - \sigma_{c0})}U_{c'c}\, e^{i(\sigma'_{c'l'} - \sigma_{c'0})}. \tag{4.6}$$

For the inelastic scattering, $U_{c'c}$ is given only by the second term. We apply one level approximation, i.e., we consider the energy region close to a resonance level λ and replace the sum of the second term for $\{\lambda JM\}$ by one term with the resonance state, and then we have

$$U_{c'c} = -i\frac{u^J_{\lambda c'}\tilde{u}^{J*}_{\lambda c}}{N^J_\lambda(E - W^J_\lambda)}. \tag{4.7}$$

We obtain cross sections for a reaction $c' \neq c$,

$$\sigma_{c'c} = g_J\frac{\pi}{k_c^2}\sum_{ll'II'}|U^J_{c'c}|^2 = g_J\frac{\pi}{k_c^2}\sum_{ll'II'}\frac{|u^J_{\lambda c'}|^2|\tilde{u}^{J*}_{\lambda c}|^2}{|N^J_\lambda|^2\{(E - E^J_\lambda)^2 + \frac{1}{4}\Gamma^2_\lambda\}}, \tag{4.8}$$

where

$$g_J = \frac{2J+1}{(2I_a+1)(2I_A+1)} \tag{4.9}$$

is the statistical factor. Now we define partial widths in the channel c' of the level λ by

$$\Gamma^J_{\lambda c'} = |u^J_{\lambda c'}|^2 = 2P_{c'l'}|\gamma^J_{\lambda c'}|^2, \tag{4.10}$$

where P_{cl} denote so-called penetration factor given by

$$P_{cl} = \frac{k_c a_c}{G^2_{cl} + F^2_{cl}}, \tag{4.11}$$

and total widths of the level λ is obtained by the sum of the partial widths,

$$\Gamma^J_\lambda = \sum_c \Gamma^J_{\lambda c}. \tag{4.12}$$

Hence, with $|N^J_\lambda| \sim 1$, we obtain the Breit-Wigner one-level formula,

$$\sigma_{c'c} \sim g_J\frac{\pi}{k_c^2}\sum_{ll'II'}\frac{\Gamma_{c'l'}\Gamma_{cI}}{\{(E - E^J_\lambda)^2 + \frac{1}{4}\Gamma^2_\lambda\}}. \tag{4.13}$$

In particular, for "on resonance", i.e., for $E = E_\lambda$, we obtain

$$U_{c'I'l',cIl}(E_\lambda) = \frac{e^{-i\phi'_{c'l'}}(-2\sqrt{2P_{c'l'}}\gamma_{c'I'l'}\sqrt{2P_{cl}}\gamma_{cIl})e^{-i\phi_{cl}}}{\Gamma^J_\lambda}, \tag{4.14}$$

where the notations are written to be more practical than in Eq.'s (4.1)~(4.4) as γ_{cIl}, but the indications for J and λ for the resonance state are omitted. ϕ_{cl} denote hard sphere scattering phase shifts, which are defined by

$$\tan\phi_{cl} = \frac{F_{cl}(k_c a_c)}{G_{cl}(k_c a_c)}. \tag{4.15}$$

To calculate $\gamma^J_{\lambda c}$ by Eq. (4.5), for Ψ^{JM}_{λ}, we adopt the model wave functions obtained by the bound-state approximation, and we take c in Eq. (4.15) to be the elastic channel, $l = J$ and c' to be single or mutual excitations, to obtain physical quantities. As for the numerical calculations, we have taken the channel radii a_c to be 9.5fm in the preliminary calculations.[15] The value is at well outside compared to the internal region. In the present paper we have corrected the tails of the radial wave functions in the concerning channels, by attaching G_{cl}'s at the smooth connecting points, because the radial behavior is gaussian-dumping type due to the bound-state approximation and harmonic approximations. The distances of the connecting points are in the range of $R = 8.3 \sim 8.8$fm. So we use a slightly larger value for a_c than those points, that is $a_c = 9.0$fm

4.2 Angular correlation

The scattering amplitudes with specified magnetic substates for the mutual 2^+ excitation are given by

$$X_{m_1 m_2}(\mathbf{k}', \mathbf{k}) = \frac{2\pi}{ik} \sum_{I'l'm'} (22 m_1 m_2 | I' m_1 + m_2)(I' l' m_1 + m_2\ m' | JM) \times i^{J-l'} e^{i(\sigma_J + \sigma'_{l'})} U^J_{I'l'} Y^*_{JM}(\hat{k}) Y_{l'm'}(\hat{k}'), \tag{4.16}$$

where $\mathbf{k}$ and $\mathbf{k}'$ denote the initial and final relative momenta between two ^{28}Si nuclei, respectively. Here we have assumed a single J resonance, and the incident(elastic) channel assignments for the collision matrices are omitted. For the single excitation, of course, we have a similar expression as the above one, by putting, for example, $I_2 = 0$ and $m_2 = 0$ into the CG coefficient $(22 m_1 m_2 | I'\ m_1 + m_2)$ of the mutual channel spin coupling. The transition amplitudes for the γ-ray emissions from the polarized nuclei are discussed by several authors (see for example Ref. [19]). For two photon emissions from the mutual excitation, the amplitudes are proportional to the scattering amplitudes and the photon emissions as

$$A^{\sigma_1\sigma_2}_{I_1 I_2} \sim \sum_{m_1 m_2} X_{m_1 m_2}(\mathbf{k}', \mathbf{k})(00|H_{\sigma_1}|I_1 m_1)(00|H_{\sigma_2}|I_2 m_2), \tag{4.17}$$

where $(00|H_\sigma|I_1 m_1)$ denote the transition matrices for γ-ray emissions, which give transition rate, i.e., by well-known perturbation theory, $2\pi/\hbar \cdot (00|H_\sigma|I_1 m_1)\rho d\Omega$ for the emission direction $d\Omega$, with ρ being level densities. In the case of the present angular correlations, photons are rapidly emitted with the half life of 700fs, which means almost all the first 2^+ states of ^{28}Si's finish their transitions into the ground states just after the decays of the resonance compounds. So the problem which we will discuss is not the magnitude of the transition rates but angular distributions of the γ-ray intensities over 4π-detectors, which were measured by EUROGAM phaseII. The γ-ray intensity distributions are given by

$$\begin{aligned}(00|H_\sigma(Im)|Im) &\sim D^I_{m\sigma}(\phi_\gamma, \theta_\gamma, 0)(IIm - m|00)(0||T(I)||I) \\ &\sim \frac{(-1)^{I-m}}{\sqrt{2I+1}} d^I_{m\sigma}(\theta_\gamma) e^{-im\phi_\gamma}.\end{aligned} \tag{4.18}$$

where σ denote right/left-hand circular polarizations of the emitted γ-rays, i.e., $\sigma = \pm 1$. After sum over them for the square of the absolute values of Eq. (4.18), we obtain γ-ray angular correlations,

$$\begin{aligned}W_{I_1 I_2}(\theta_1, \phi_1; \theta_2, \phi_2) &\equiv \sum_{\sigma_1 \sigma_2} |A^{\sigma_1 \sigma_2}_{I_1 I_2}|^2 \\ &= \sum_{\sigma_1 \sigma_2 m_1 m_2 m_1' m_2'} X_{m_1 m_2}(\mathbf{k}', \mathbf{k}) X^*_{m_1' m_2'}(\mathbf{k}', \mathbf{k}) \\ &\qquad \times (00|H_{\sigma_1}|I_1 m_1)(00|H_{\sigma_1}|I_1 m_1')^* \\ &\qquad \times (00|H_{\sigma_2}|I_2 m_2)(00|H_{\sigma_2}|I_2 m_2')^*,\end{aligned} \tag{4.19}$$

where θ_i and ϕ_i denote angles of photon directions. In the experiment, only one of two emitted photons is detected in most cases, even with EUROGAM. Therefore we take an average over the angles of one photon (θ_2, ϕ_2), and so we practically integrate the last line of Eq. (19), which turns out to be proportional to $\delta_{m_2 m_2'}$. Hence the intensity distributions are given by

$$\begin{aligned}W_{I_1 I_2}(\theta_1, \phi_1) \sim \sum_{m_1 m_1', m_2} & X_{m_1 m_2}(\mathbf{k}', \mathbf{k}) X^*_{m_1' m_2}(\mathbf{k}', \mathbf{k}) \\ & (00|H_{\sigma_1}|I_1 m_1)(00|H_{\sigma_1}|I_1 m_1')^*\end{aligned} \tag{4.20}$$

Furthermore note also that the intensities of the detectors are averaged over the azimuthal angle ϕ_γ in the final experimental results, which simplifies the comparison to the data. By taking the average, we obtain only diagonal contributions

P_m, and thus the normalized angular correlations are expressed as

$$W(\theta_\gamma) = \sum_m P_m W_m(\theta_\gamma), \tag{4.21}$$

where P_m's are the probabilities in the correlated m magnetic substates of one of two fragments, i.e., are given by

$$P_m \sim \sum_{m_2} |X_{mm_2}(\mathbf{k}', \mathbf{k})|^2. \tag{4.22}$$

$W_m(\theta_\gamma)$ denote the $E2$ γ-ray angular distributions,

$$W_m(\theta_\gamma) = \frac{1}{2} \sum_{\sigma=\pm 1} (\sqrt{5/4\pi} d^2_{m\sigma}(\theta_\gamma))^2, \tag{4.23}$$

the intensity patterns of which are well-known (see for example Ref. [30]). The patterns are displayed in Fig. 11 for convenience for readers.

In order to calculate the angular correlations, we specify the initial beam direction $\mathbf{k}$ and the final fragments direction $\mathbf{k}'$ in the scattering amplitudes of Eq. (4.16). The final direction $\mathbf{k}'$ was taken to be θ_{cm} in the experiment. The IReS 4π γ-data were processed (integrated on the angle ϕ) for the given three quantization axes (shown in Fig. 12); in system (a), the z-axis is taken to be in the beam direction, in (b) normal to the scattering plane and in (c) in the fragment direction.

Another important point for the analysis is a width of the particle detectors. Position-sensitive detectors are set aligned along the reaction plane to measure the angular distributions, vertical acceptance of which is $\pm 4°$. For fragment-fragment-γ coincidence, the event was selected in which the both ^{28}Si's were detected in the range of $\theta_{cm} = 90° \pm 7°$. So we have to take the detector-width into account. One may think that the width is enough small to neglect the effect. His idea is correct for usual low partial waves, but this is not the case. In extremely high spin resonances such as partial $L \sim 38$, the oscillations of the partial waves are very rapid as are seen Fig. 2, where the angle differences between the maximum to zero amplitude are seen only about 2°. Hence we need to take an average over the detector area. Such an effect is indispensably important for the correlation in the single excitation channel, as will be discussed in the following section. Because due to the Bohr condition we have no $m = \pm 1$ component at exact $\theta_{cm} = 90°$,

but actually we have rather large $m = \pm 1$ component as seen in (a)-axes in the experimental data[7] (see Fig. 17). Since the orbital angular momentum vector is almost perpendicular to the reaction plane, the waves propagate rapidly oscillating along the reaction plane, and rather slowly varies along the vertical direction. Therefore we need to integrate on only one dimension, i.e., only along the reaction plane (interval $\theta_{cm} = \pm 7°$). To be sure, we compared the results between those with one-dimensional integration and with two-dimensional one. Actually the differences are very small as less than 1% of the total amounts.

§5. Results and Discussion

First we inspect the angular correlation data for the mutual excitation channel[15]. Figure 12 displays γ-ray intensities from the first excited state to the ground state, in the mutual inelastic channel $(2_1^+, 2_1^+)$ decays. The 4π γ-data are shown for the given three quantization axes; in the panel (a) the z-axis is taken to be in the beam direction, in (b) normal to the scattering plane and in (c) in the fragment direction. Theoretical intensities of γ-rays emitted by the ^{28}Si fragments in the decay of the molecular ground state ($J = 38$) are also given in Fig. 12, indicated by dotted lines, which are seen to be in quite good agreement with the data in all the three quantization axes (a), (b) and (c). The above theoretical results are obtained preliminary for the final $\mathbf{k}'$ direction of $\theta_{cm} = 90°$, i.e., without the average over the detector width. As is shown in the following, the nature of the spin alignments in the mutual channel receives essentially no change by averaging over the detector width. In Fig. 12 K-mixing was done with the parameter $b = 1.26$ in Eq. (3.20), the magnitude of which is consistent with asymmetry of the ^{28}Si + ^{28}Si molecular ground-state configurations, while we adopt a value $b = 1.41$ in the following. This is because characteristic features of the data such as "m=0" in (b) become indistinct by the average, and therefore to fit the data we have shifted the magnitude of K-mixing strengths to be slightly larger.

We examine theoretical results for typical molecular states. Before that, it is better to look the results of $b = 2.0$ shown in Fig. 13, for the molecular ground state again (the same configuration as in Fig. 12, except for the value b), where all the internal motions are zero-point ones. One can see the results are almost the same as the preliminary ones of $\theta_{cm} = 90°$. By a detail look, one may find even a better fit in the (c)-system. Next, for the other modes, the first is the results

for $K = 0$ molecular ground state (no K-mixing) shown in Fig. 14, in which we can know the effect of K-mixing. In the middle panel (b), "m=2" is seen to be dominant but "m=0" component is also contained, and so we feel not so bad. The calculated "m=0" probability is, however, rather small as $P(m = 0) = 0.15$, while the data suggests the value 0.46. In the other panels the fits are seen to be not good, although the whole tendency of the three panels is roughly in accordance with the experimental data. Secondly figure 15 displays angular correlations for the butterfly mode, and finally figure 16 displays those for the twisting mode ($\nu \sim 4$). All those theoretical results are apparently much different from the data. The characteristic features of the results are existence of dominant "m=2" substates, i.e., in (c) of the butterfly mode in Fig. 15 and in (a) of the twisting mode in Fig. 16, respectively. This means that the spin vectors are on the reaction plane; spin vectors are parallel to the fragment direction in the butterfly mode and to the beam direction in the twisting mode, respectively. However those angular correlations are seen to be inconsistent with the data, for example, as we see "m=1" patterns in (a) and (b) of the butterfly mode. By the comparisons, it is clear that the molecular ground state with K-mixing at high spins is very good candidate for the resonance, and the other modes fail to be. One may expect that results for the butterfly mode are favorable for the "m=0" characteristic, because spin orientations are perpendicular to the normal axis. However, more precisely, "m=0" means "symmetric around the normal axis", which is satisfied by neither of excited states such as butterfly nor twisting with well-defined direction of the spin on the reaction plane.

One may think that the above results are not intuitive or confusing, because for example, for the twisting mode the ^{28}Si nuclei rotate around the molecular z'-axis by the definition, and then the spin vectors are parallel to the molecular z'-axis axis, which would be towards the fragment direction after the resonance decay. However the theoretical results suggest that the spin vectors of the twisting mode are dominantly parallel to the beam direction, and so one might feel the spin directions are strange or even incorrect. The situation is similar for the butterfly mode, where the spin vectors would be on the reaction plane by K-mixing but are perpendicular to the molecular z'-axis. Such an intuition is correct in usual nuclear reaction, where the di-nuclear fragments come into the detectors along the relative vector after the resonance decays. In high spin resonances, however, the expectation would be denied due to extremely high speed rotational motion,

the direction of which is perpendicular to the relative vector as everyone sees in raindrop motions splashed from an rapidly rotating umbrella. For a test on motions of the ^{28}Si nuclei after decay, we calculated classical orbits and obtained the angle from the relative direction to be about 70° for $J = 38$. As a confirmation we calculated angular correlations with $J = 8$, where the results turn out to be opposite spin directions compared with $J = 38$, i.e., "m=2" dominance appears in (c) for the twisting mode.

Lets move to the single excitation channel $(2_1^+, 0_1^+)$, the experimental angular correlations of which are displayed in Fig. 17[7]. Surprisingly those of the single channel are seen to be almost the same as those for the mutual channel. As already mentioned in section 4, to reproduce those angular correlation data we have to take average over the detector width. Figure 18 dispays theoretical results obtained with the same K-mixing strength $b = 1.41$ and one-dimensional integration as done in the mutual channel. The all the three panels show excellent agreements with the data. The value of $m = \pm 1$ magnetic substate probability in (a)-axes calculated by the integration is 0.31, which is never obtained from the final ^{28}Si direction of $\theta_{cm} = 90°$. By the molecular ground state we can reproduce dominant "m=0" substate in (b) as well as in the mutual channel.

§6. Summary

The energetically favored configuration of an oblate-oblate dinuclear system such as $^{28}\mathrm{Si} + {}^{28}\mathrm{Si}$ is the parallel equator-equator one, as examined in section 3, with the shape of the whole system like two pancakes touching each other side-to-side. At a given angular momentum J, this configuration rotates in a triaxial way approximately about the axis corresponding to the largest moment of inertia in the state with the lowest energy. Therefore the whole system rotates about the normal to the plane defined by the two pancake-like nuclei. We have developed the molecular model to include such rotations by K-mixing, which is described in subsection 3.2. The spins of the ^{28}Si fragments are thus in this plane since no rotation can occur about ^{28}Si symmetry axes. This result is in agreement with the lack of strong alignment observed in the angular distribution data. Thus such a rotation or reaction mechanism is expected to occur in the very high spin resonances.

We have examined several molecular modes to know which of them agrees with

the characteristic angular correlation data "m=0". None of the normal modes are not in agreement with "m=0", because the excited states such as butterfly and twisting have specified spin directions on the reaction plane, respectively, i.e., "m=2" in their own directions. Only K-mixed molecular ground state has been selected as a good candidate.

The structure of the K-mixed molecular ground state should be called as "wobbling mode", which is due to the tri-axial deformation of the ^{28}Si + ^{28}Si stable configuration. K-rotational modes such as tilting or wobbling have been discussed for deep inelastic scattering processes[31], but up to now the appearance of the mode in a resonance phenomena has not been known. As an experimental technique, the angular correlations is a powerful tool for the study of nuclear structures of heavy-ion resonances, and further progress is strongly desired.

Acknowledgements

The authors thank Drs. C. Beck and F. Haas for stimulating discussions in their collaborations.

References

1) R.R. Betts, *Proc. 4th Intern. Conf. on Clustering Aspects of Nuclear Structure and Nuclear Reactions, Chester, 1984*, eds. J.S. Lilley and M.A. Nagarajan (D. Reidel, Dordrecht, 1985), p. 133.
2) R.R. Betts, S.B. DiCenzo and J.F. Petersen, Phys. Rev. Lett. **43** (1979), 253.
3) R.R. Betts, S.B. DiCenzo and J.F. Petersen, Phys. Lett. **100B** (1981), 117.
4) R.R. Betts, B.B. Back and B.G. Glagola, Phys. Rev. Lett. **47** (1981), 23. Mg+Mg
5) R.W. Zurmühle et al., Phys. Lett. **129B** (1983), 384.
6) S. Saini, R.R. Betts, R.W. Zurmühle, P.H. Kutt and B.K. Dichter, Phys. Lett. **B185** (1987), 316.
7) C. Beck, R. Nouicer, et al., Phys. Rev. **C63** (2000), 014607.
8) Y. Abe, Y. Kondō and T. Matsuse, Prog. Theor. Phys. **Suppl. No.68** (1980), Chapter IV, p.303, and *references therein.*
9) T. Bengtsson, M. Faber, M. Ploszajczak, I. Ragnarsson and S. Åberg, Preprint Lund-MPh-84/01 (1984) and also in Ref. 3), and M. Faber and M.

Ploszajczak, Physica Scripta **24** (1981), 189.
10) R.A. Broglia, C.H. Dasso, H. Esbensen and A. Winther, Nucl. Phys. **A349** (1980), 496.
11) R. Maass and W. Scheid, Phys. Lett. **B202** (1988), 26.
12) E. Uegaki and Y. Abe, Phys. Lett. **B231** (1989), 28.
13) E. Uegaki and Y. Abe, Prog. Theor. Phys. **90** (1993), 615.
14) E. Uegaki and Y. Abe, Phys. Lett. **B340** (1994), 143.
15) R. Nouicer, C. Beck, et al., Phys. Rev. **C60** (1999), 041303.
16) D. Konnerth et al., *Proc. Fifth Intern. Conf. on Clustering Aspects in Nuclear and Subnuclear Systems, Kyoto, 1988*; J. Phys. Soc. Jpn. **58** (1989) Suppl., p. 325.
17) A.H. Wuosmaa et al., Phys. Rev. Lett. **58** (1987), 1312; Phys. Rev. **C41** (1990), 2666.
18) A. M. Lain and R. G. Thomas, Rev. Mod. Phys. **30** (1958), 257.
19) F. Rybicki, T. Tamura and G.R. Satchler, Nucl. Phys. **A146** (1970) 659.
20) J. Blocki, J. Randrup, J. Swiatecki and C.F. Tsang, Ann. of Phys. **105** (1977) 427.
21) M. El-Azab Farid and G.R. Satchler, Nucl. Phys. **A438** (1985) 525.
22) G.R. Satchler and W.G. Love, Phys. Rep. **55** (1979), 183.
23) For example, C.R. Howell et al., Phys. Rev. **C38** (1988) 1552.
24) P.M. Endt, Nucl. Phys. **A521** (1990), 1.
25) A. Bohr and B.R. Mottelson, *Nuclear Structure vol. I,* (Benjamin, New York, 1969), p. 158.
26) T. Takatsuka, Prog. Theor. Phys. **73** (1985), 1043.
27) J.P. Blaizot, Phys. Rep. **64** (1980), 171.
28) A. Bohr and B.R. Mottelson, *Nuclear Structure vol. II* (Benjamin, Massachusetts, 1975), p. 175.
29) Y.R. Shimizu, private communication
S.W. $^{16}O + ^{16}O$ degård, *et al.*, Phys. Rev. Lett. **86** (2001) 5866.
30) J. de Boer et al., *Proc. Intern. School Phys., Enrico Fermi Course LXXVII, Nuclear Structure and Heavy-Ion Collisions* (North-Holland, Amsterdam, 1981), p. 655.
31) J. Randrup, Nucl. Phys. **A447** (1985), 133c. See also L. Moretto, G. Peaslee and Wozniak, Nucl. Phys. **A502** (1989), 453c.

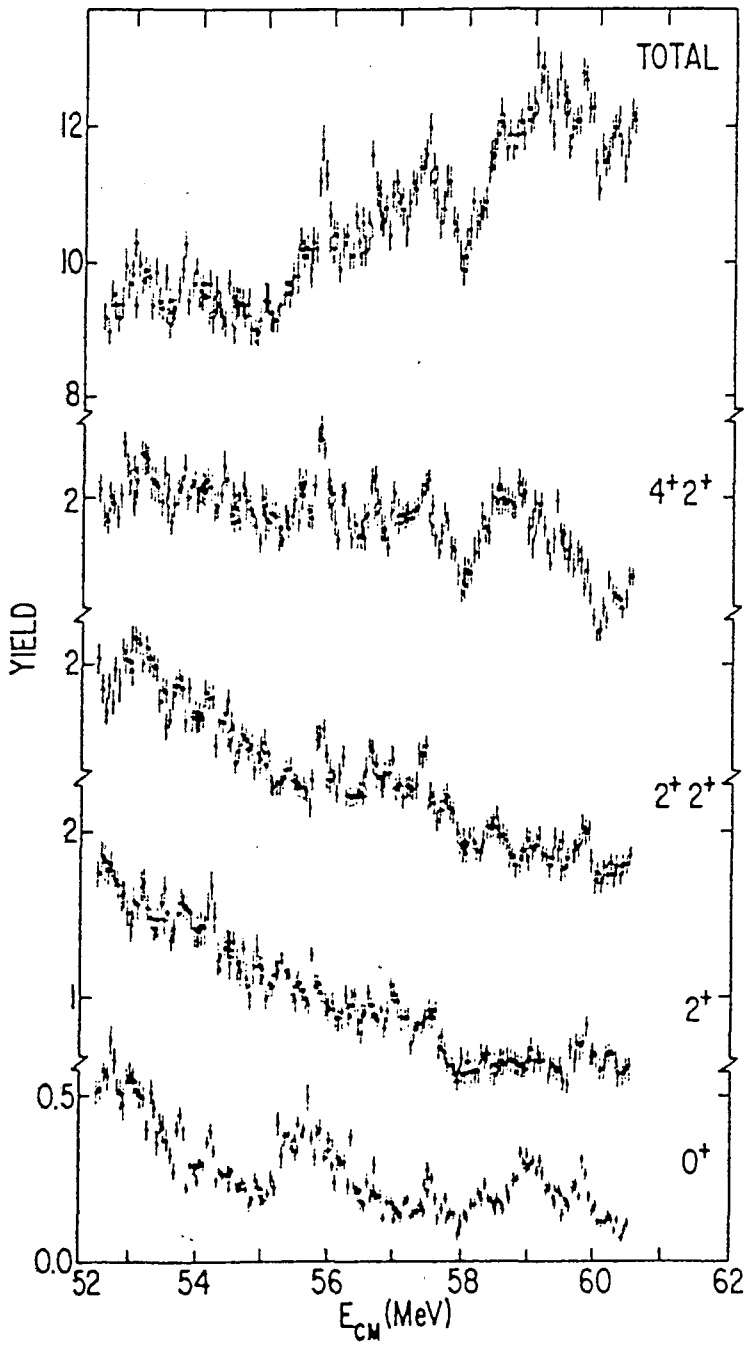

Fig. 1. Experimental excitation functions for ^{28}Si + ^{28}Si reactions. Angle-integrated yields of the elastic scattering, 2^+, mutual 2^+ and mutual $(4^+, 2^+)$ excitations shown as a function of $E_{\mathrm{c.m.}}$. The top part of the figure shows the total yield in the spectrum.

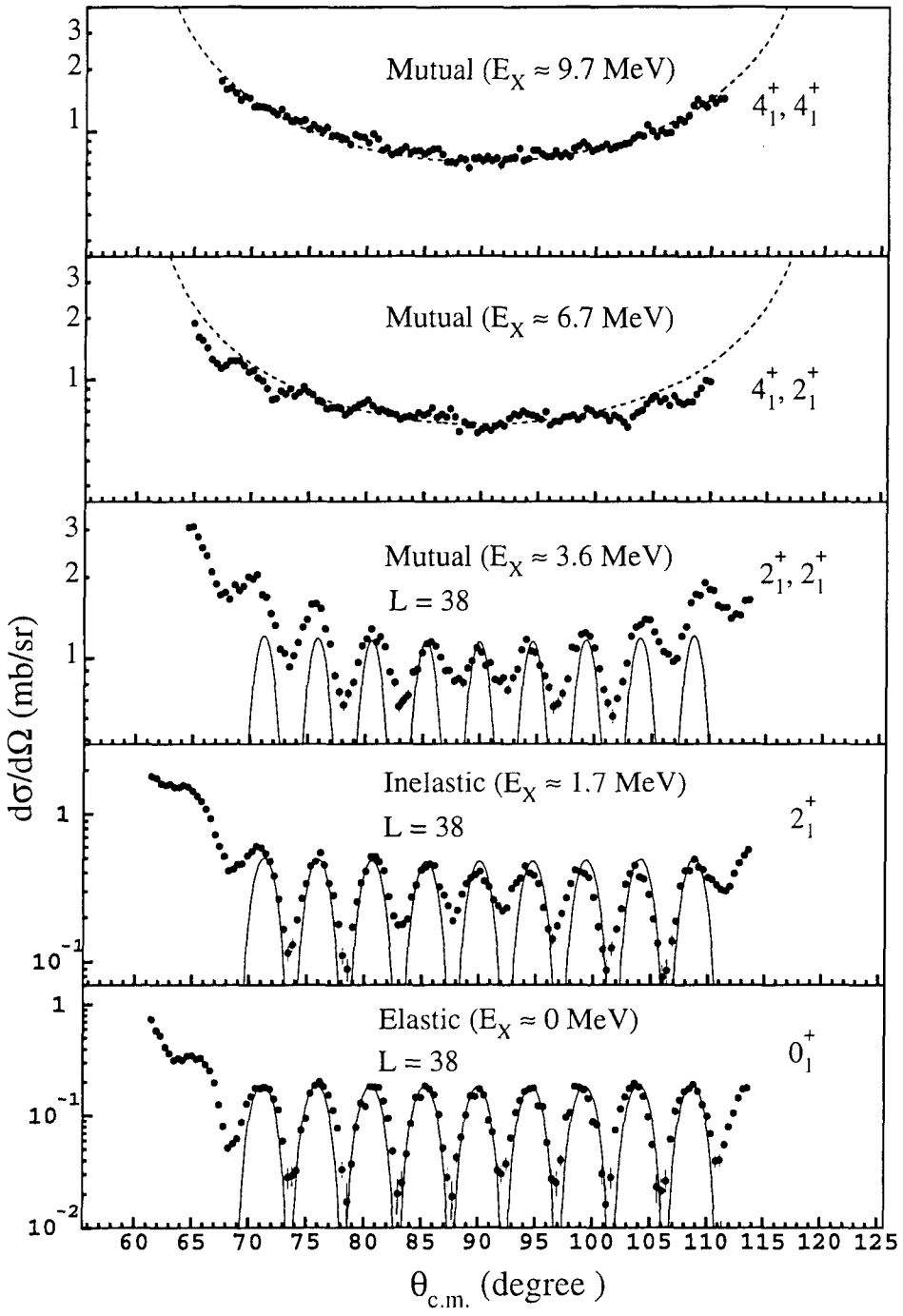

Fig. 2. Experimental angular distributions for the elastic and inelastic scattering for $^{28}Si + ^{28}Si$ at $E_{c.m.} = 55.8$MeV. Solid curves show L=38 Legendre fits for comparison.

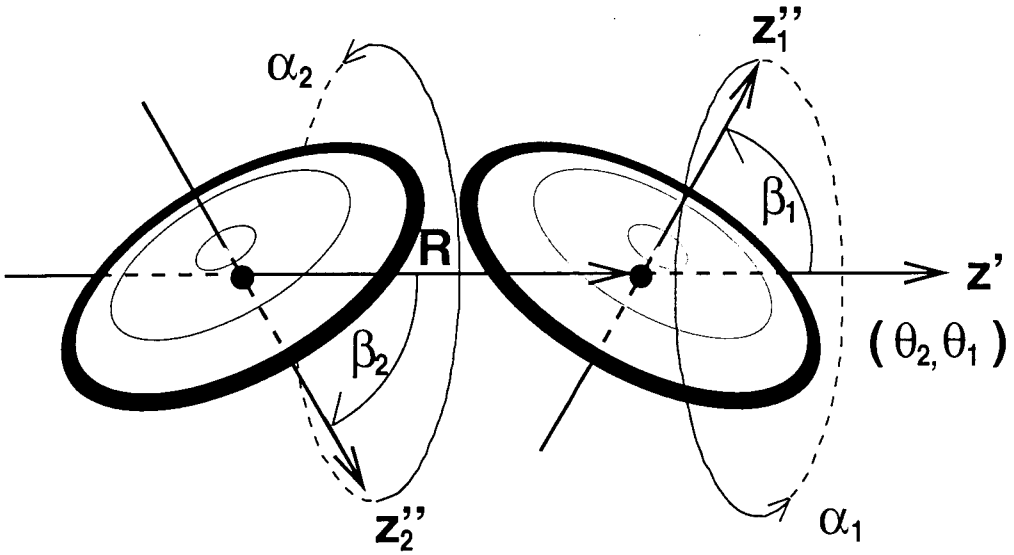

$$\theta_3 = (\alpha_1 + \alpha_2)/2$$

$$\alpha = (\alpha_1 - \alpha_2)/2$$

Fig. 3. Di-nuclear configuration and the coordinates in the rotating molecular frame for a oblate-oblate system. Molecular z'-axis and seven degrees of freedom of the system are displayed.

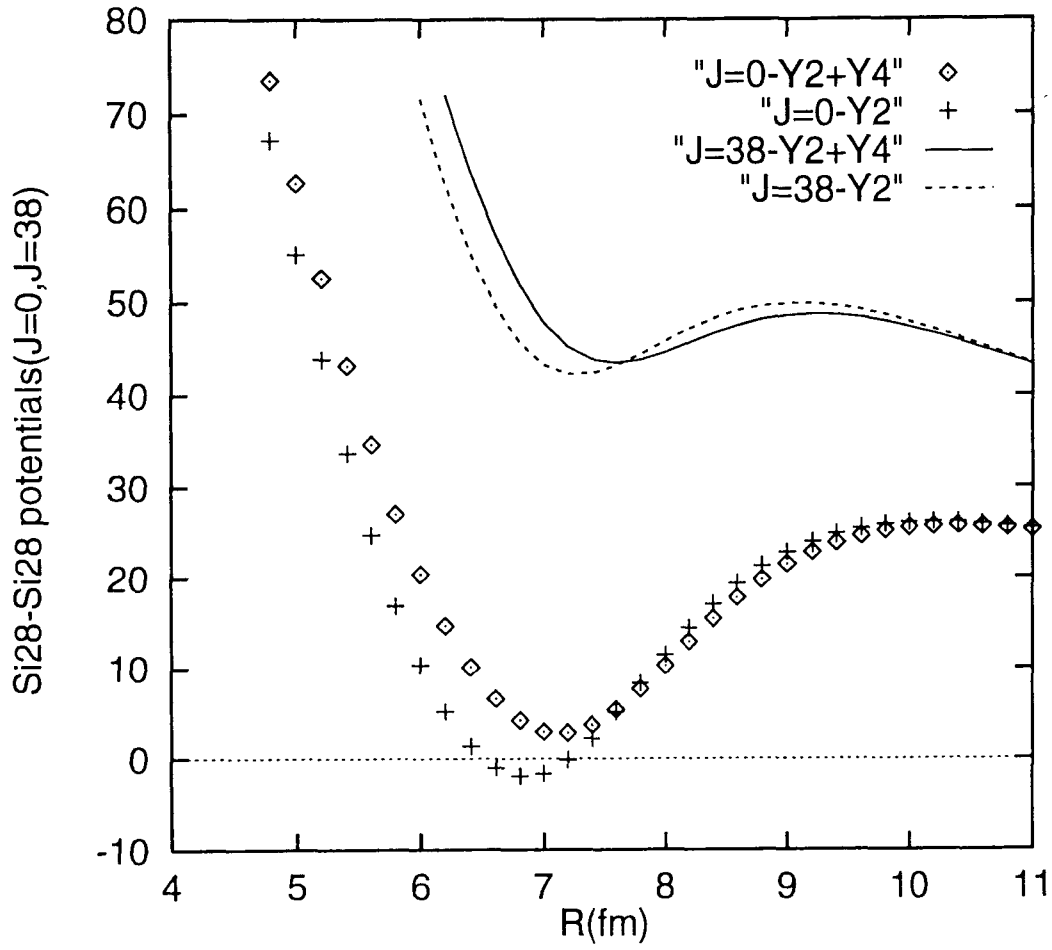

Fig. 4. The radial forms of the effective potentials in the equator-equator configuration of ^{28}Si + ^{28}Si, $V_{JK} = V_{\rm int}(R, \pi/2, \pi/2, \pi/2) + T'_{\rm rot}(J, K)$ with spin $J = 0$ and $J = 38$ with $K = 0$ are shown. Labels Y2 and Y2+Y4 indicate the type of the deformation, where the latter inculdes hexadecapole moment.

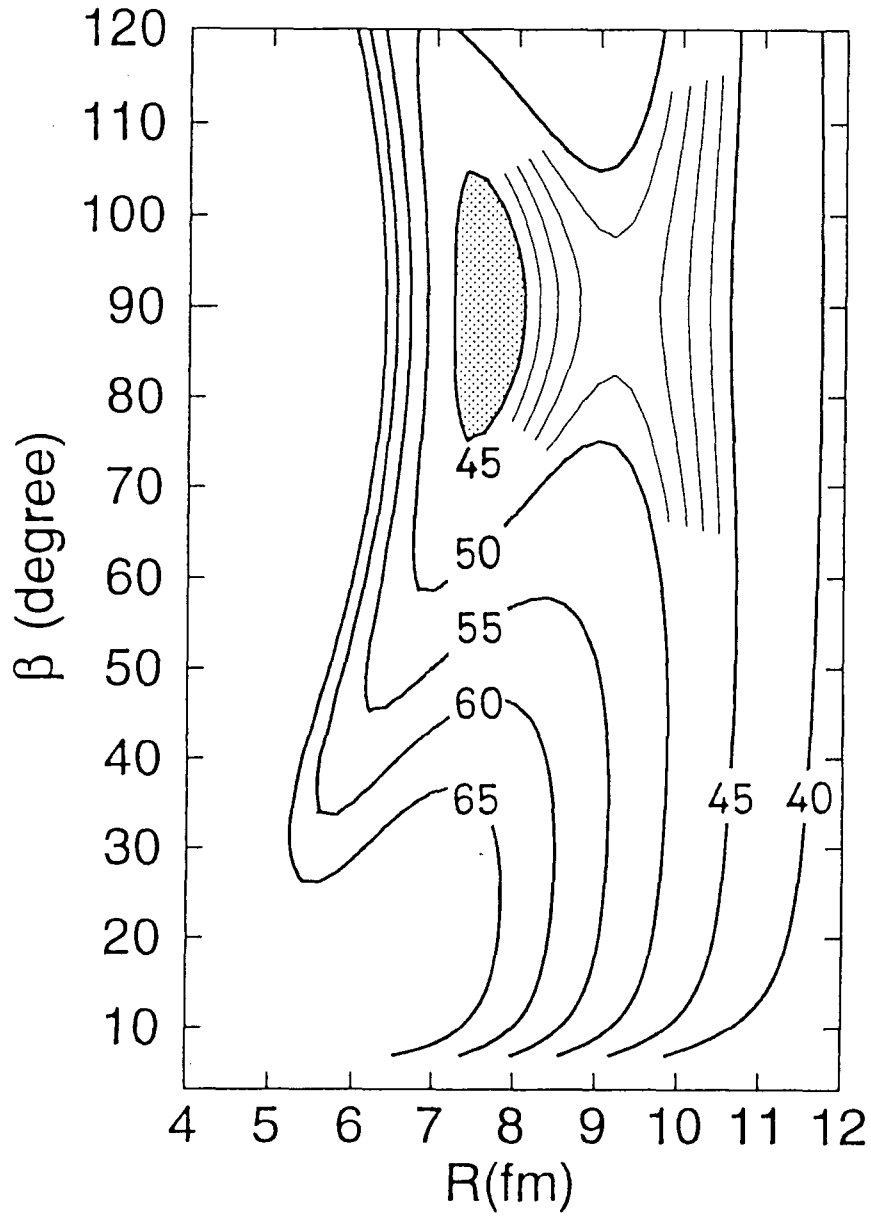

Fig. 5. An R-$\beta(\beta_1 = \beta_2, \alpha = \pi/2)$ energy surface for ^{28}Si + ^{28}Si system, effective potential energy V_{JK} with $J = 38$ and $K = 0$ is displayed, A local enegy minimum exists at $R = 7.6$fm. Contours are in MeV.

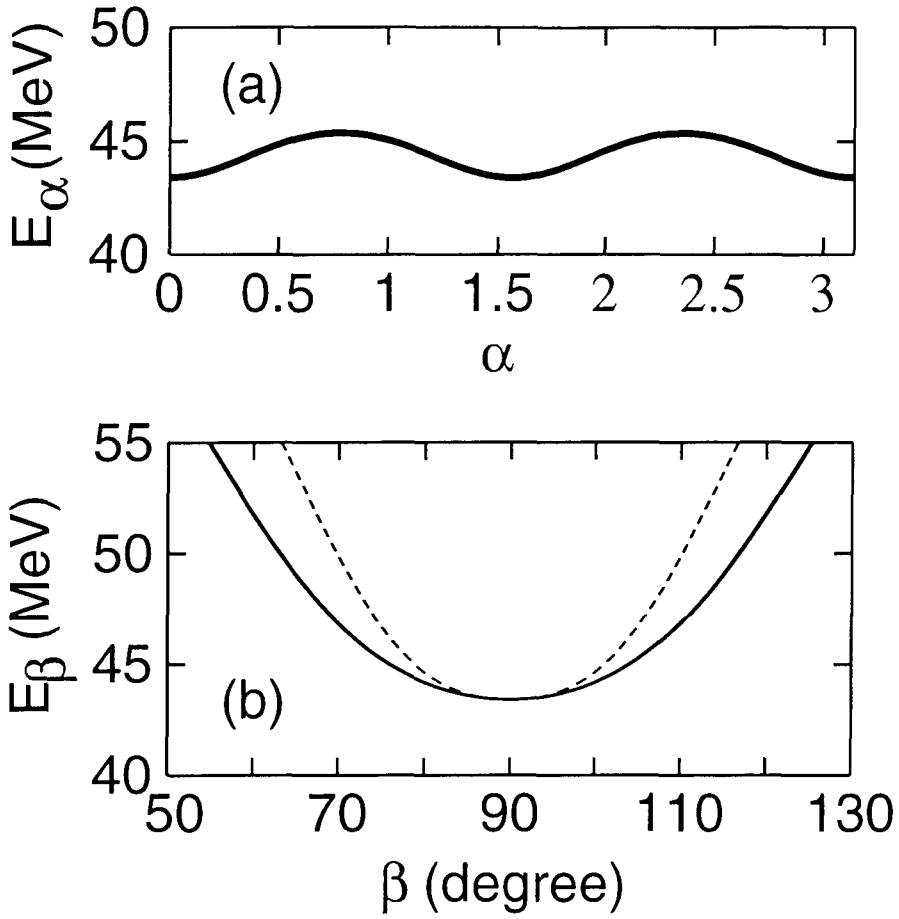

Fig. 6. (a) α-dependence of the effective potential V_{JK} with $J = 38$ and $K = 0$, for the E-E configuration at $R = R_e = 7.6$fm. (b) V_{JK} versus $\beta = \beta_1 = \beta_2$ at $\alpha = 0$ and at $\alpha = \pi/2$, which are displayed by dashed and solid lines, respectively.

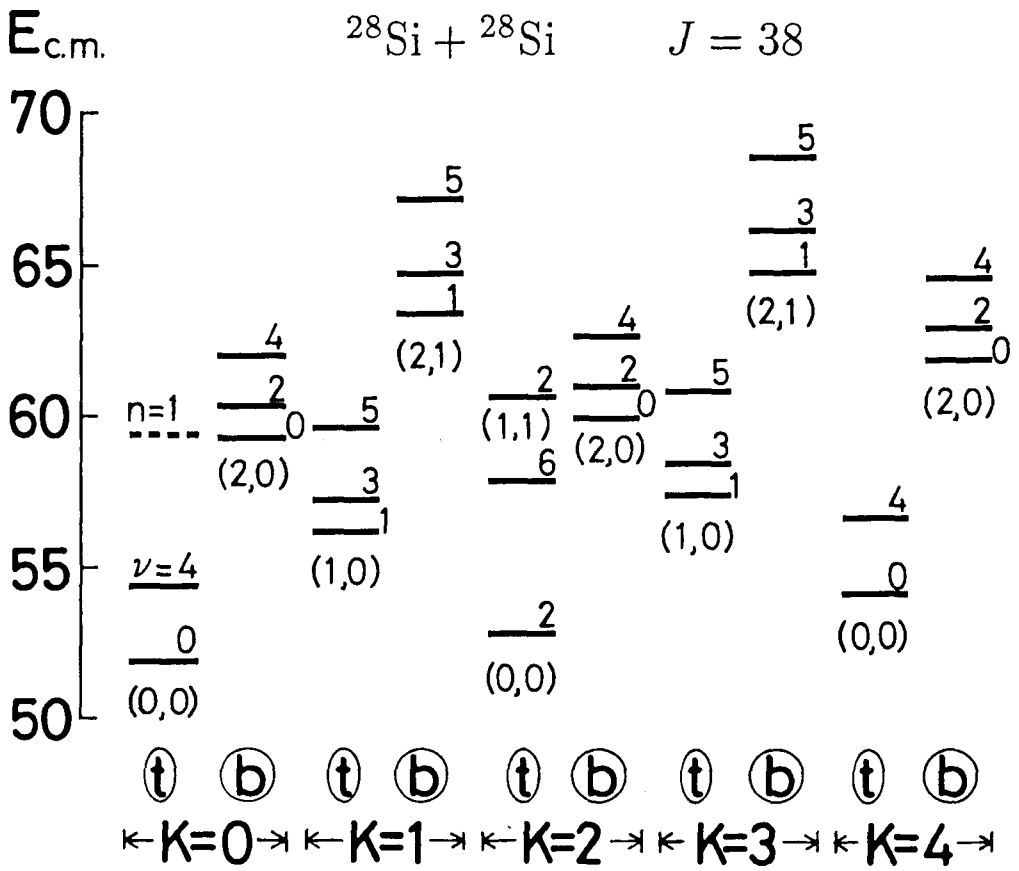

Fig. 7. Molecular normal modes for ^{28}Si + ^{28}Si system for $J = 38$. The quantum states are specified by $(n, n_+, n_-, K, (\nu, \pi_\alpha))$, where $n = 0$ except for one level($n = 1, \nu = 0$) displayed with dashed line. The quanta (n_+, n_-) of β-motions are given below the levels, and K at the bottom. ν for α-motion is given at the upper right-hand-side of the levels. (t) and (b) marks are assigned in the lower part of the figure, which indicate twisting rotational and butterfly modes, respectively.

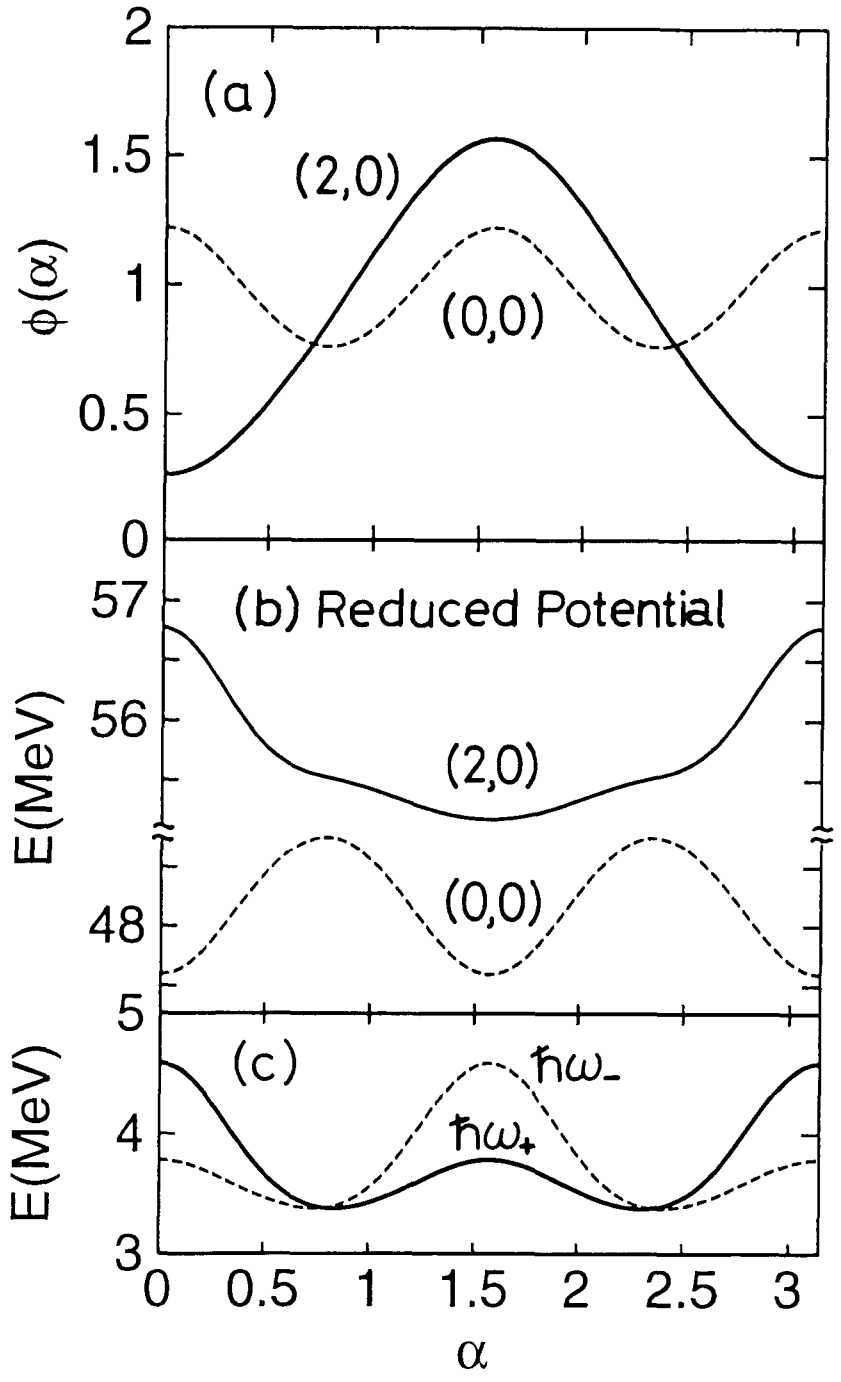

Fig. 8. (a) Wave functions for α-motion with $\nu = 0$, with zero-point oscillation $(0,0)$ and butterfly excitation $(2,0)$ for β-degrees, respectively, are displayed for $J = 38$ and $K = 0$. (b) The reduced α-potential $V_{JK}(R_e, \alpha, \frac{\pi}{2}, \frac{\pi}{2}) + E^{\beta}_{n_+,n_-}(\alpha)$. (c) α-dependence of β-energy quanta $\hbar\omega_{\pm}$.

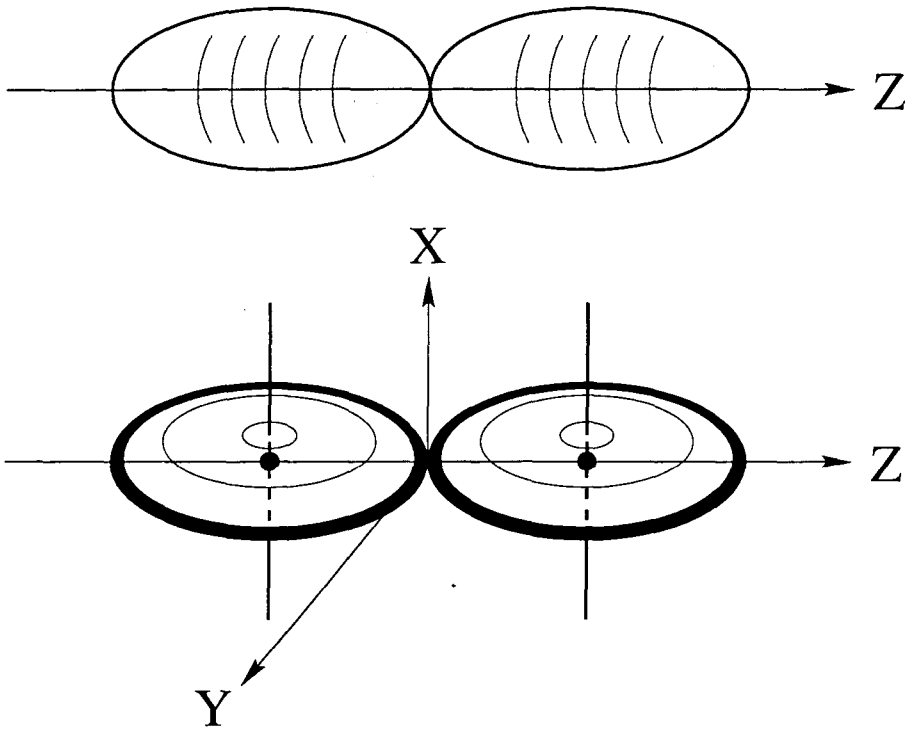

Fig. 9. Equilibrium configurations of di-nuclear systems. Upper panel is for $^{24}Mg + ^{24}Mg$ and lower panel for $^{28}Si + ^{28}Si$.

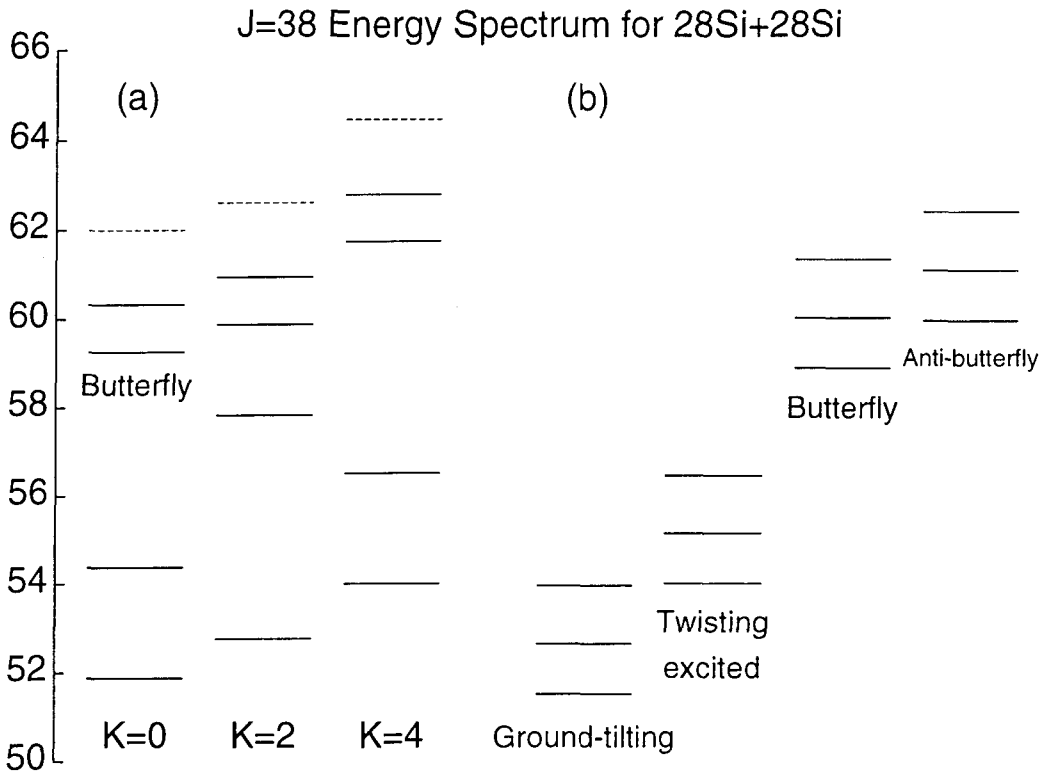

Fig. 10. Energy spectra for $J = 38$ levels of $^{28}Si + ^{28}Si$. (a) Without K-mixing from Fig. 7 and (b) with K-mixing.

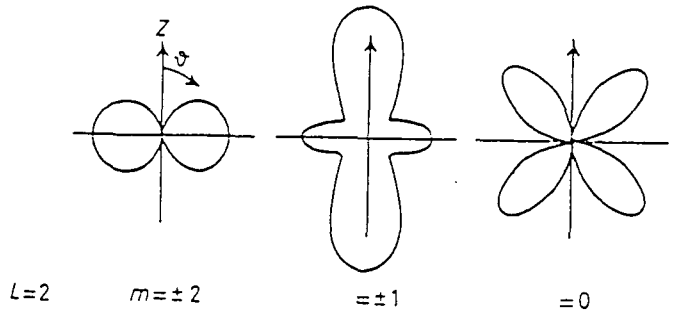

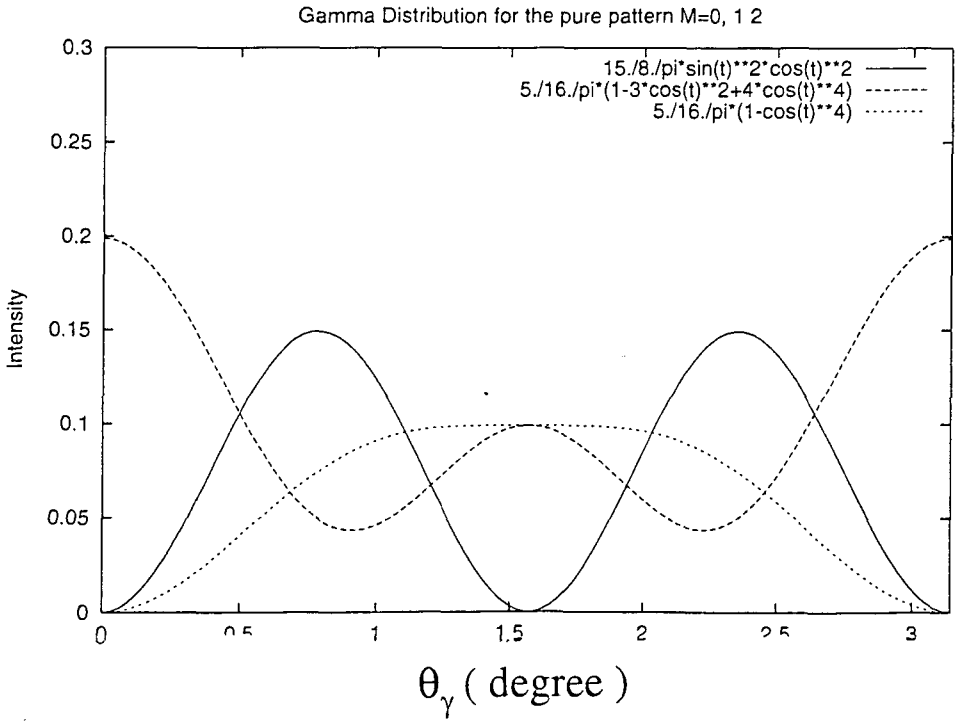

Fig. 11. Angular distributions of $E2$ γ-ray emissions. The upper panel displays intensities by the distance from the origin, which lower panel shows the same thing with the polar angle θ in the abscissa.

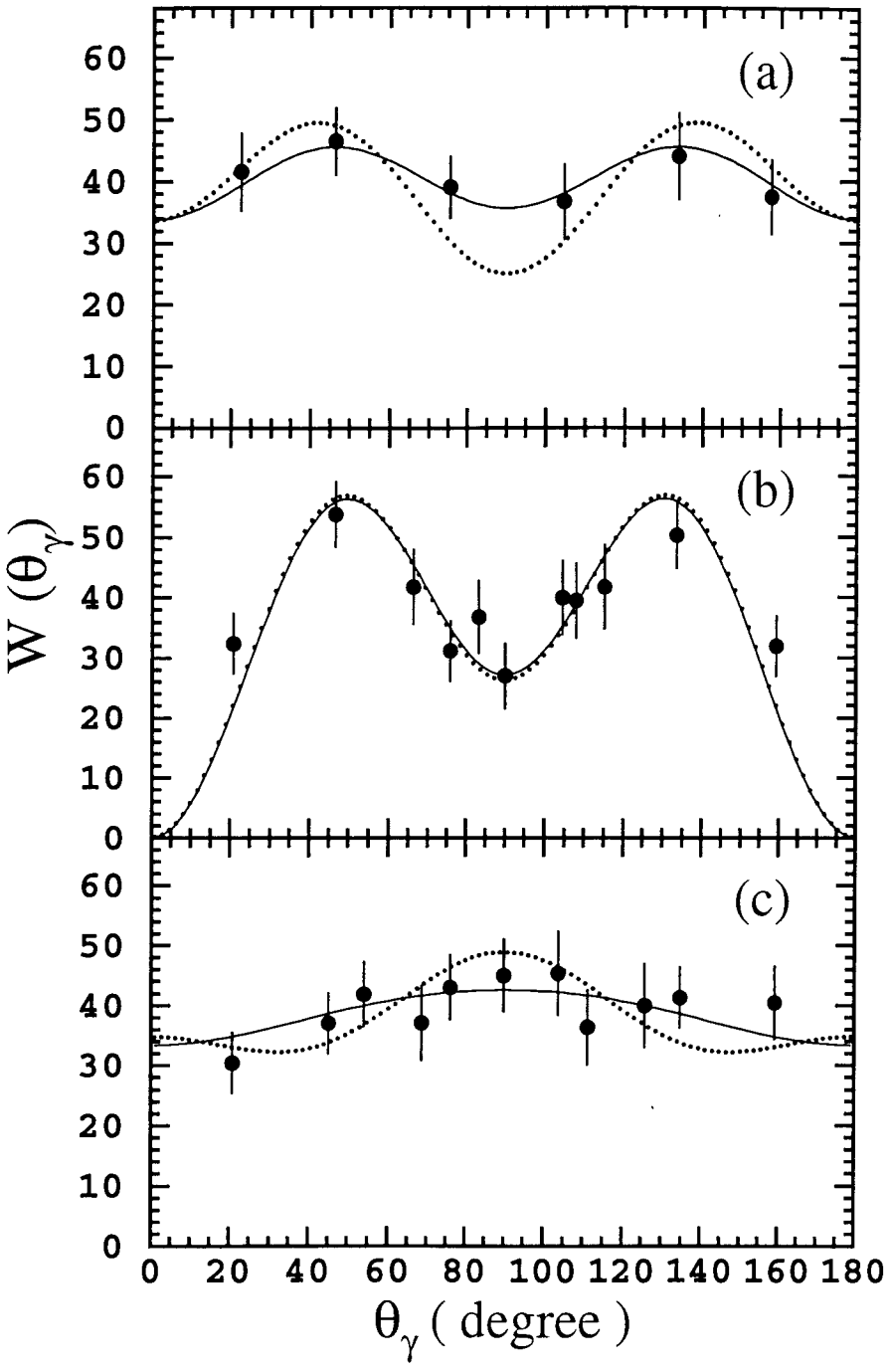

Fig. 12. γ-rays intensities obtained from particle-particle-γ coincident measurements for the mutual excitation channel. Solid curves show χ^2-fits. Dotted lines show the theoretical prediction obtained by the molecular model with wobbling mode (K-mixings). For the quantization axes in three panels, see text.

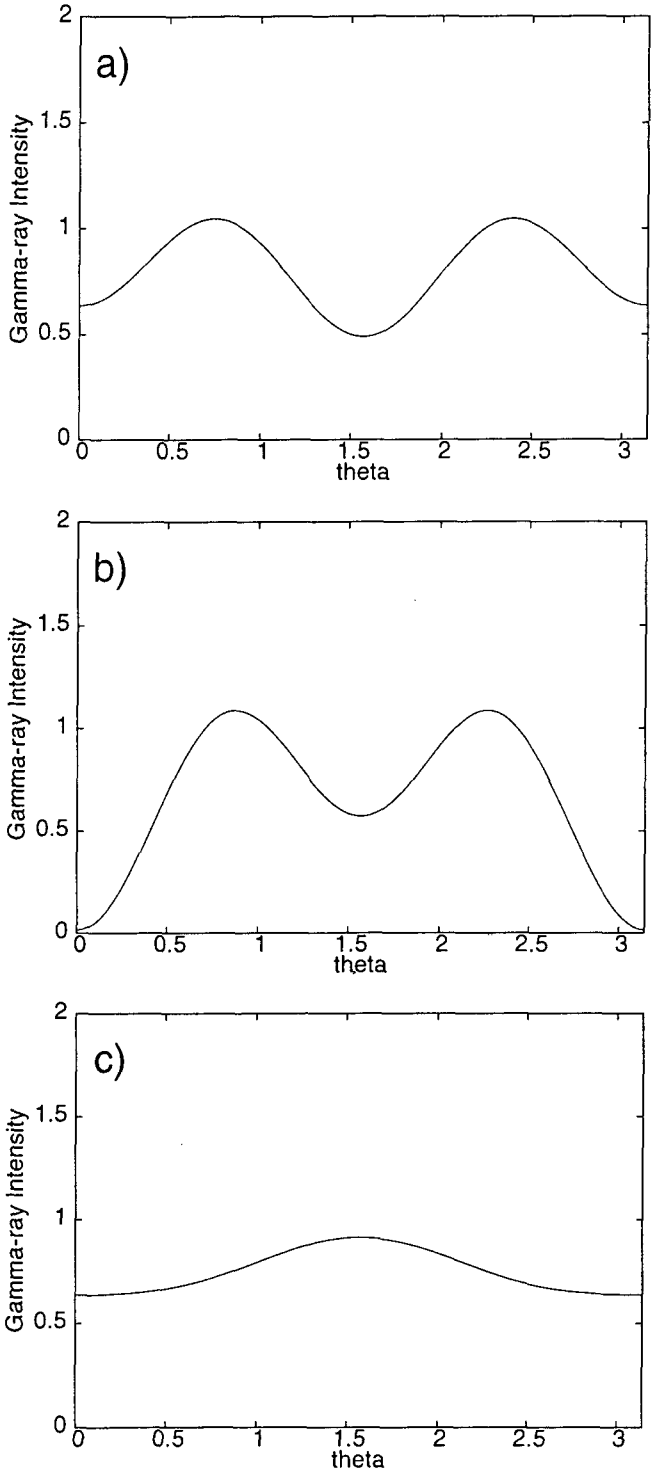

Fig. 13. γ-ray intensities for the angular correlations in the mutual excitation channel, for the molecular ground state. The data are displayed by three quantization axes, (a) the z-axis in the beam direction, (b) normal to the scattering plane and (c) in the fragment direction, respectively.

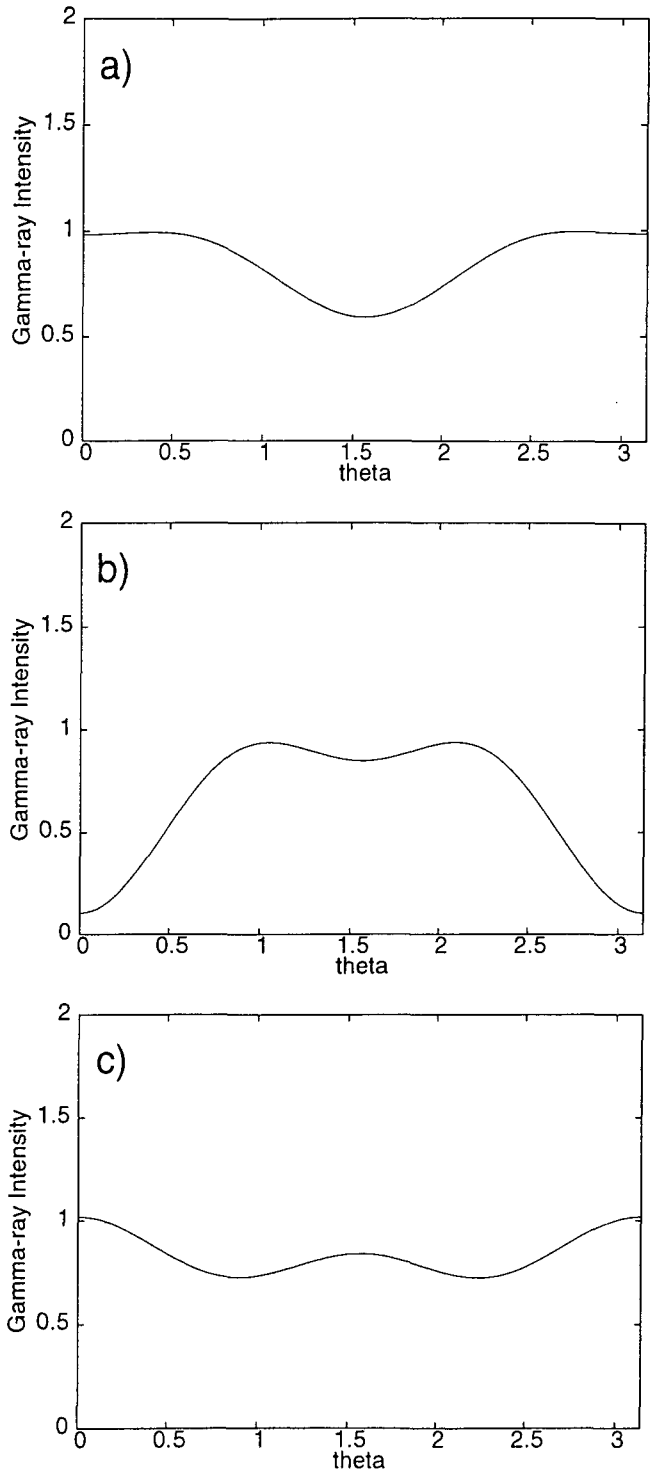

Fig. 14. γ-ray intensities for the angular correlations in the mutual excitation channel, for the $K = 0$ molecular ground state (without K-mixing). With three quantization axes, (a), (b) and (c) explained in the text and the same as in Fig. 13.

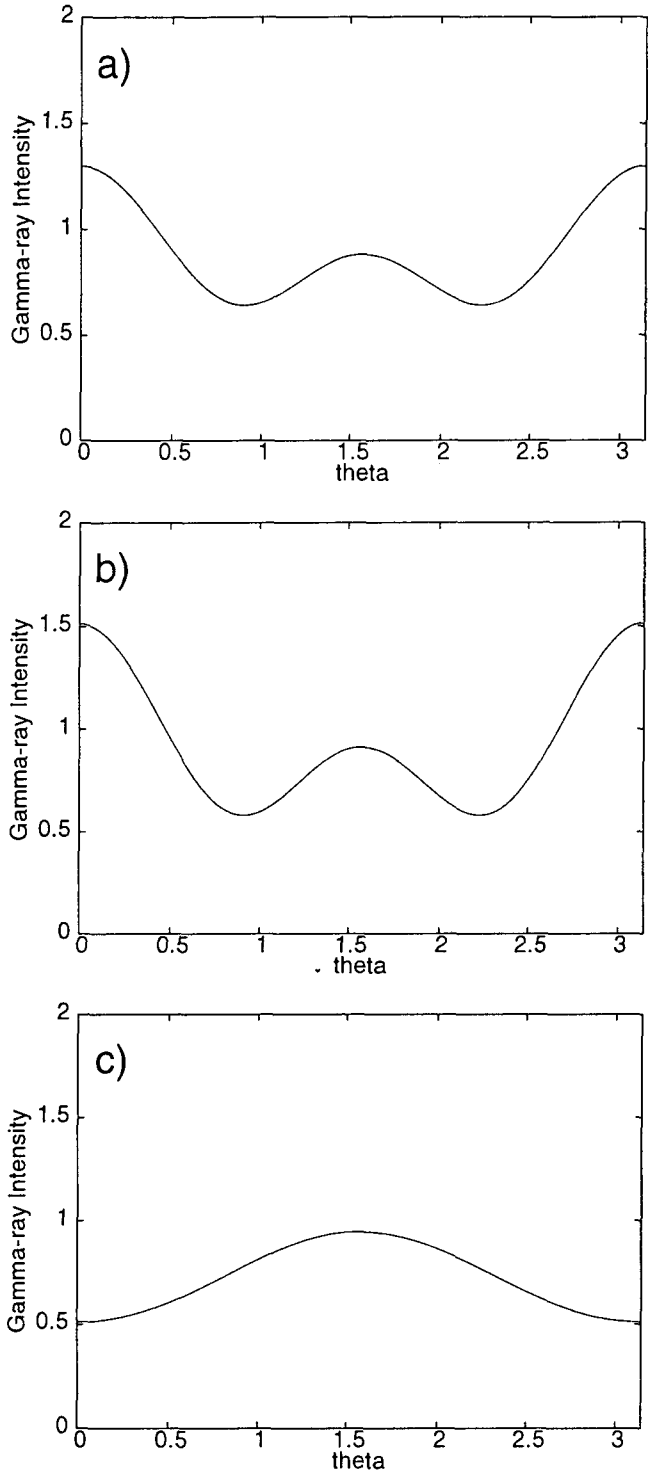

Fig. 15. γ-ray intensities for the angular correlations in the mutual excitation channel, for the butterfly mode. With three quantization axes, (a), (b) and (c) explained in the text and the same as in Fig. 13.

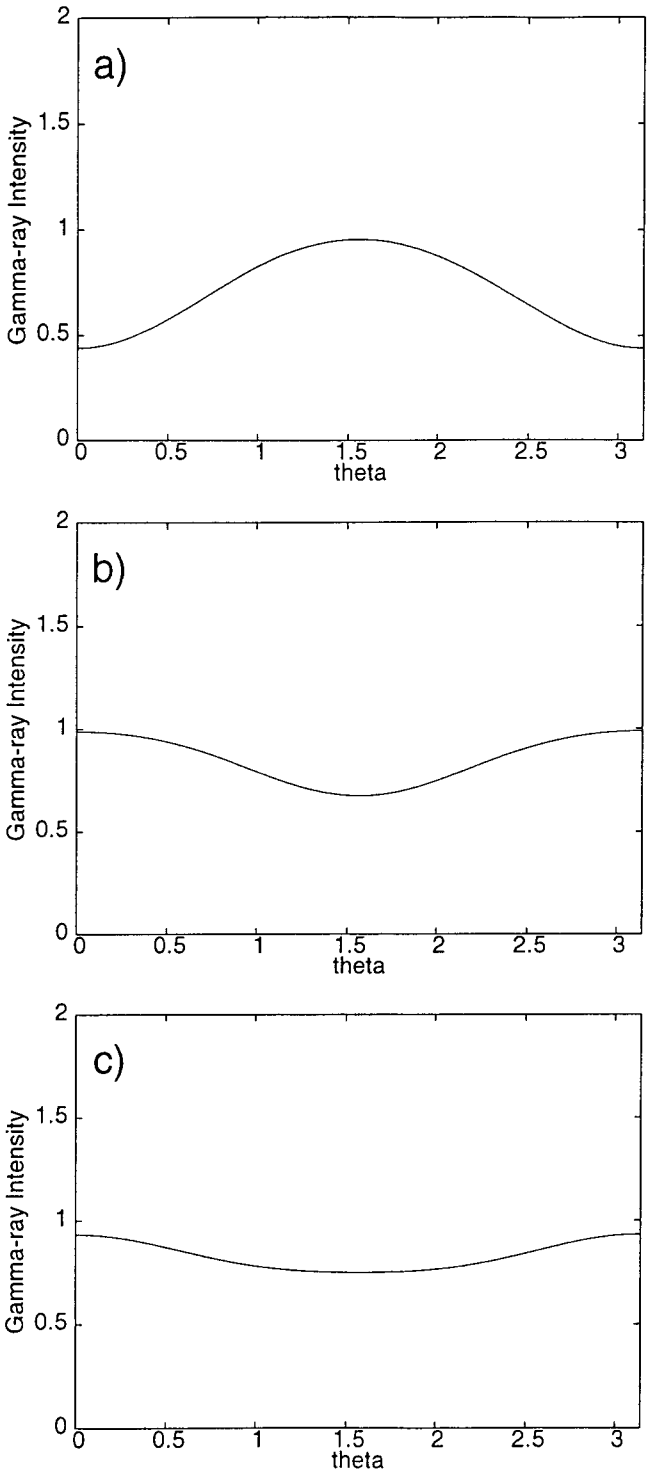

Fig. 16. γ-ray intensities for the angular correlations in the mutual excitation channel, for the twisting mode. With three quantization axes, (a), (b) and (c) explained in the text and the same as in Fig. 13.

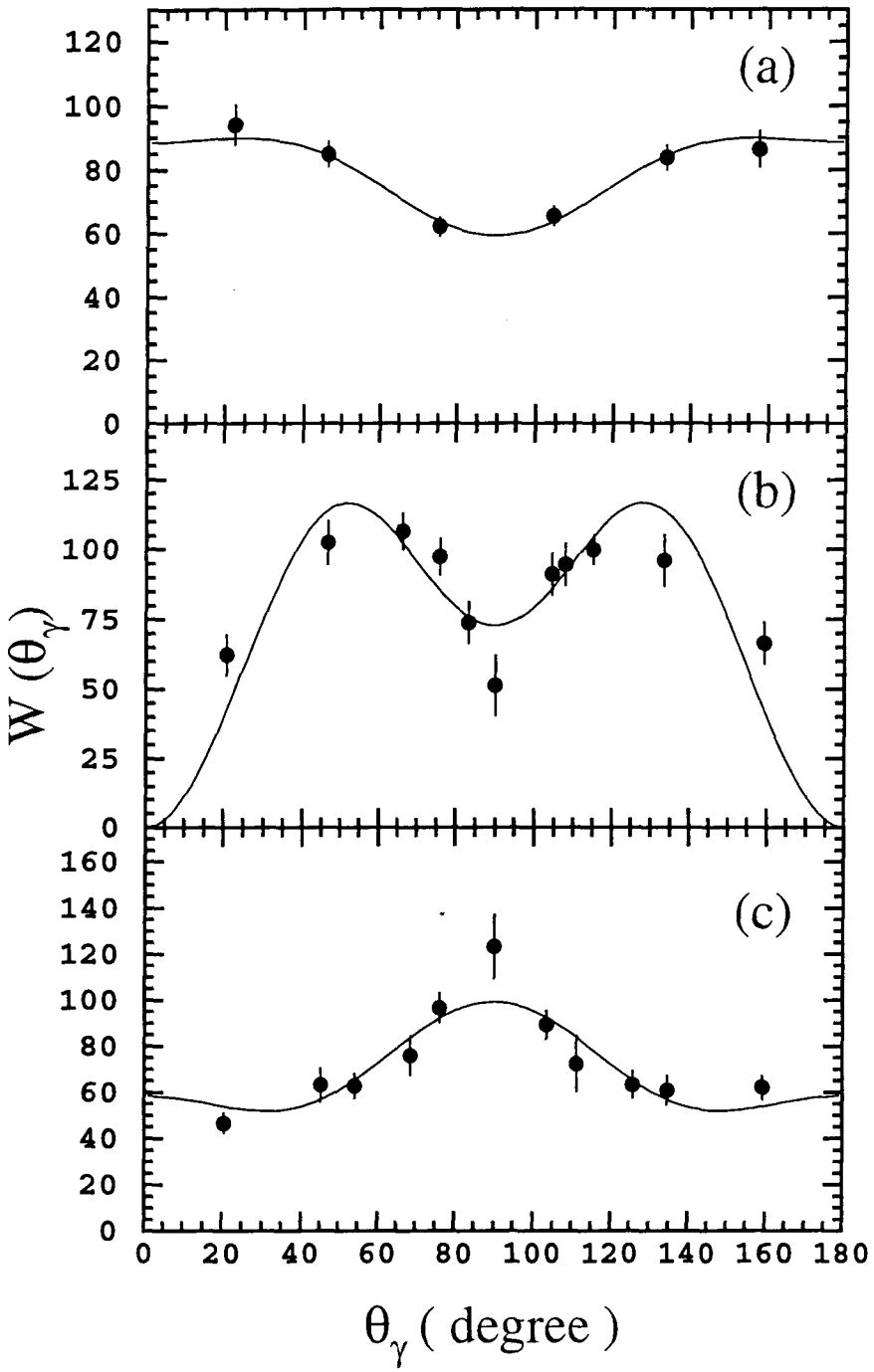

Fig. 17. γ-rays intensities obtained from particle-particle-γ coincident measurements for the single excitation channel. Solid curves show χ^2-fits. For the quantization axes in three panels, see text.

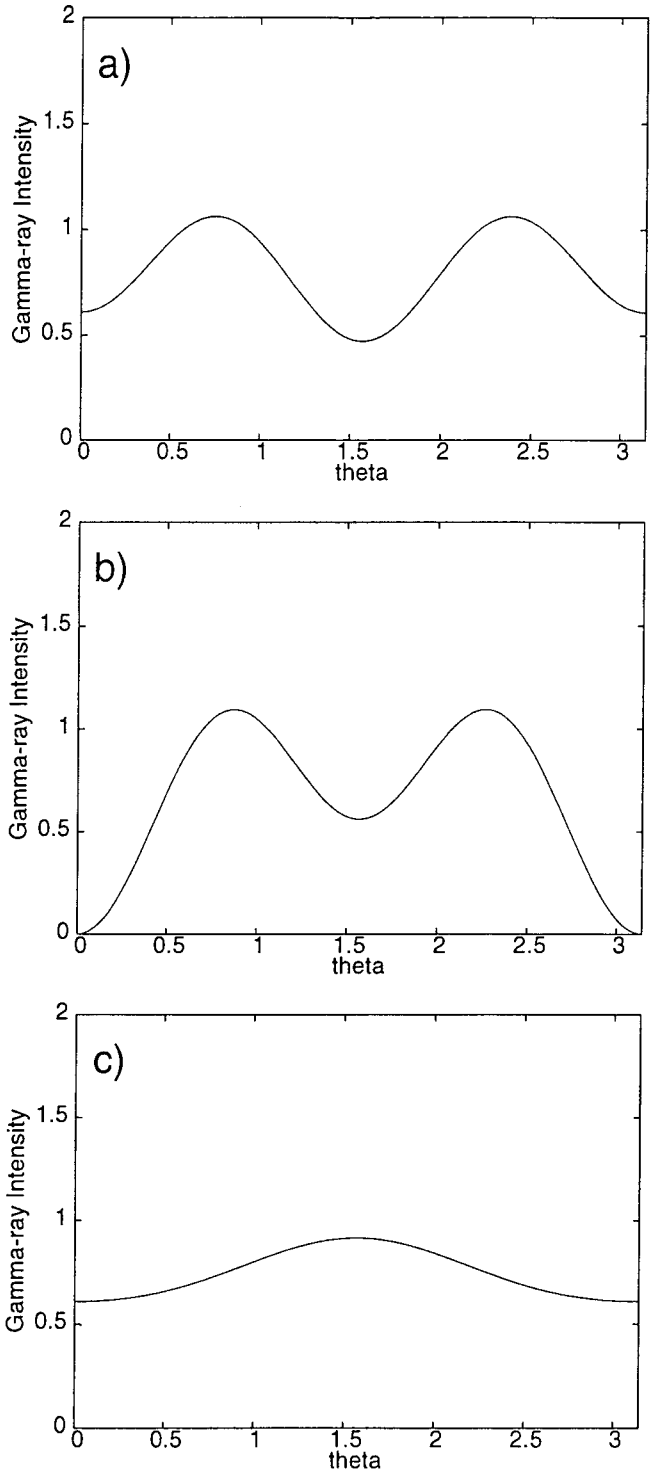

Fig. 18. γ-ray intensities for the angular correlations in the single excitation channel, for the molecular ground state. With three quantization axes, (a), (b) and (c) explained in the text and the same as in Fig. 13.

Proceedings of the Symposium on Nuclear Clusters (2002) 163–170

Symposium on Nuclear Clusters
Rauischholzhausen, Germany
5–9 August 2002

Angular Correlations in ^{28}Si + ^{28}Si Resonances

E. Uegaki[1] and Y. Abe[2]

[1] Department of Mechanical Engineering, Akita University
Akita 010-8502, Japan

[2] Yukawa Institute for Theoretical Physics, Kyoto University
Kyoto 606-8502, Japan

Abstract. Recent particle–particle–γ coincident measurements on a ^{28}Si+^{28}Si resonance have suggested "vanishing spin alignments". New analyses of the spin alignments with a molecular model are presented. It is clarified that due to a triaxial deformation of the total system a wobbling mode (K-mixing) appears to give rise to spin disalignment.

Keywords: heavy-ion resonances, molecular model, angular correlation
PACS: 25.70.Ef, 21.60.Gx, 23.20.En

1. Introduction

Angular correlation measurements recently made with 4π gamma detectors has given rise to much progress in study of molecular resonances [1]. Now, characteristic features of the experiments are summarized in the following three points which have to be explained theoretically: 1) narrow resonance structures correlating among the elastic and inelastic channels, 2) angular distributions in the elastic and inelastic channels, 3) angular correlations between emerging fragments ^{28}Si and gamma rays emitted from the fragments. The second characteristic indicates a dominance of the partial wave $L = J$. Figure 1 shows the angular distributions for the elastic and inelastic channels 2^+, $(2^+, 2^+)$, respectively, on the resonance at $E_{\rm CM} = 55.8$ MeV. The oscillating patterns are found to be in good agreement with $L = 38$, which suggests $L = J = 38$ dominance in the resonance, namely, *misalignments* of the fragment spins. And the third one indicates "$m = 0$" spin orientations of the fragments in the normal to the reaction plane. Thus, the latter two quantities suggest a disalignment between the orbital angular momentum and the fragment spins. In the present paper we take up the third characteristic, namely, "$m = 0$" newly explored by the angular correlations, and examine which molecular mode is a good candidate for the resonance state.

ISBN 963 206 299 X

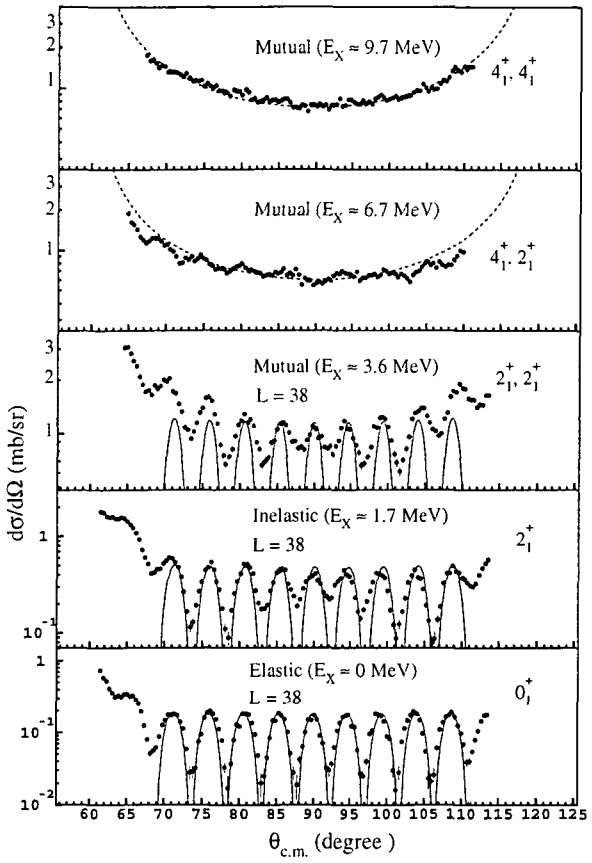

Fig. 1. Experimental angular distributions for the elastic and inelastic scattering for $^{28}Si + ^{28}Si$ at $E_{CM} = 55.8$ MeV. Solid curves show $L = 38$ Legendre fits for comparison.

Gamma rays from the first excited state of ^{28}Si to the ground state have been measured in coincidence with two ^{28}Si nuclei detected at $\theta_{CM} = 90°$. Figure 2 displays γ-ray intensities of the mutual inelastic channel $(2_1^+, 2_1^+)$ decays for three quantization axes from 4π data, where in the panel (a) the z axis is taken to be in the beam direction, in (b) normal to the scattering plane and in (c) in the fragment direction. The angular correlation in (b) shows characteristic "$m = 0$" pattern, which suggests that the fragment spins $\mathbf{I}_1$ and $\mathbf{I}_2$ are on the scattering plane, and is consistent with the misalignments observed in ^{28}Si angular distributions. Those features are much different from $^{12}C + ^{12}C$ and $^{24}Mg + ^{24}Mg$ systems which exhibit spin alignments [2]. Thus, the data are expected to provide a good test for the model.

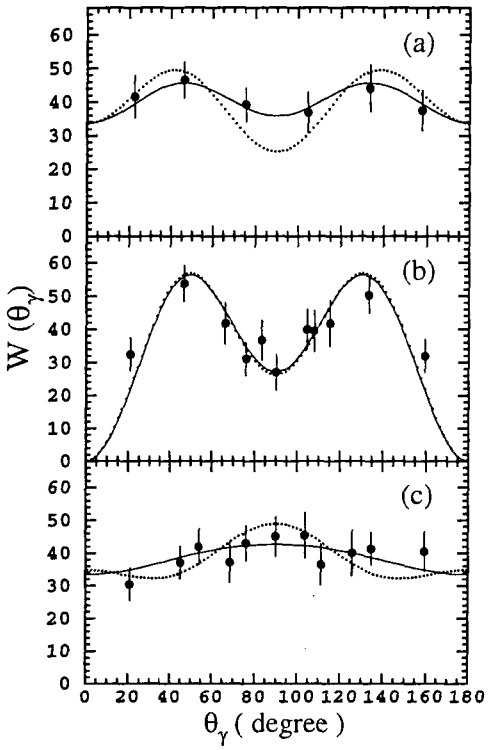

Fig. 2. γ-ray intensities obtained from particle–particle–γ coincident measurements. Solid curves show χ^2-fits. Dotted lines show the theoretical prediction obtained by the molecular model with wobbling mode (K-mixings). For the quantization axes in the three panels, see text.

2. Molecular Model

2.1. Di-nuclear structure of $^{28}Si + ^{28}Si$ system

With extremely high spins such as $30 \sim 40\,\hbar$, stable di-nuclear configurations tend to be "elongated systems by the strong centrifugal force". In the prolate–prolate systems (^{24}Mg + ^{24}Mg), a stable configuration is the pole-to-pole one, while in the oblate–oblate systems (^{28}Si + ^{28}Si), it is an equator-to-equator one displayed in Fig. 3a. By the molecular model, the authors have attempted to solve normal modes around the equilibrium [3]. Seven degrees of freedom $(q_i) = (\theta_1, \theta_2, \theta_3, R, \alpha, \beta_1, \beta_2)$ illustrated in Fig. 3b are considered with the assumption of a constant deformation and axial symmetry of the constituent nuclei, for simplicity. Consistently with the coordinate system, we introduce a rotation–vibration-type wave function as basis,

$$\Psi_\lambda \sim D^J_{MK}(\theta_i)\chi_K(R, \alpha, \beta_1, \beta_2)\,, \tag{1}$$

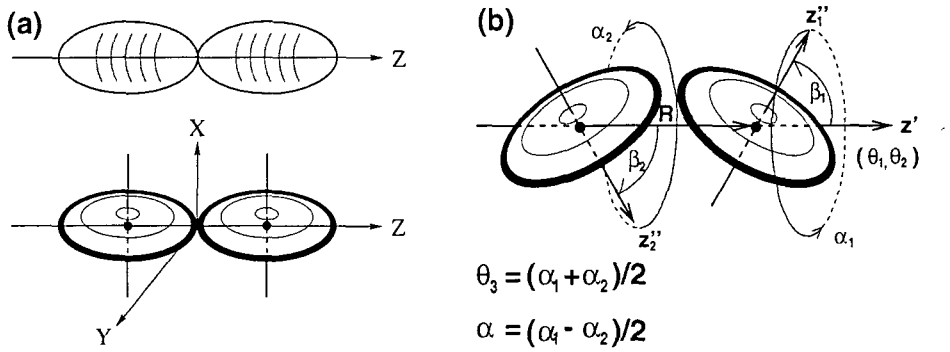

Fig. 3. (a) Equilibrium configurations of di-nuclear systems. Upper panel is for ^{24}Mg + ^{24}Mg and lower panel for ^{28}Si + ^{28}Si. (b) Coordinate system of ^{28}Si + ^{28}Si.

where χ_K describes internal motions. Dynamics of the internal motions have been solved around the equilibrium and various normal modes such as butterfly vibrations have been obtained [3,4]. An example of the spectrum with spin $J = 38$ is shown in Fig. 4a.

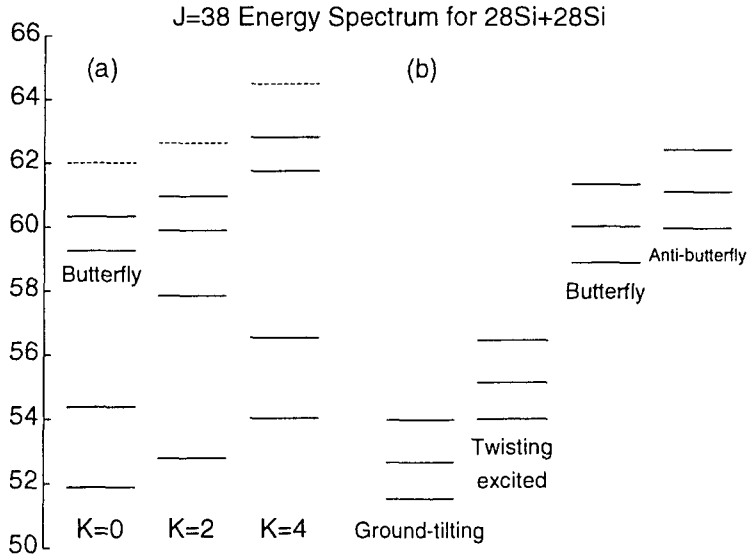

Fig. 4. Energy spectra for $J = 38$ levels of ^{28}Si + ^{28}Si. Without K-mixing (a) and with K-mixing (b).

Characteristic features of the spectrum are series of low-energy K-rotational excitations due to axial asymmetry around the molecular z axis, which is in contrast with ^{24}Mg + ^{24}Mg case [3, 5]. One can understand the reason immediately from Fig. 3a, where the upper configuration has axial symmetry as a whole, but the lower one has axial asymmetry. Approximately a triaxial system rotates around the axis with the maximum moments of inertia. By the definition of the axes in the lower panel of Fig. 3a, we have $I_x > I_y \gg I_z$. Thus two pancake-like objects (^{28}Si) touching side-by-side rotate around the x axis which is normal to the reaction plane. And then the spin orientations of the two ^{28}Si nuclei are on the plane in consistency with "$m = 0$", because the nuclei rotate around the axes perpendicular to their symmetry axes.

In order to obtain an accurate description of this triaxial rotator, as it is well known for polyatomic molecules, we diagonalize the Hamiltonian with an asymmetric inertia tensor, which gives rise to a mixing of K-projections of the total spin J [6]. The resultant motion should be called "wobbling mode" [7]. In the high spin limit ($K/J \sim 0$), the diagonalization in the K-space is found to be equivalent to solving a differential equation of the harmonic oscillator with parameters given by the moments of inertia. Thereby, the solution is a Gaussian, or a Gaussian multiplied by an Hermite polynomial,

$$f_n(K) = H_n\left(\frac{K}{b}\right)\exp\left[-\frac{1}{2}\left(\frac{K}{b}\right)^2\right], \tag{2}$$

with the width of $b = (2J^2 I_K/\Delta)^{1/4}$, where $I_K^{-1} = I_z^{-1} - I_{\rm av}^{-1}$ and $\Delta^{-1} = I_y^{-1} - I_{\rm av}^{-1}$ with $I_{\rm av}^{-1} = \frac{1}{2}(I_x^{-1} + I_y^{-1})$. The resultant energy spectrum is displayed in Fig. 4b compared with the spectrum without K-mixings in Fig. 4a. To calculate angular correlations we introduce a wobbling mode by the lowest state $f_0(K)$ of Eq. (2),

$$\Psi_\lambda^{JM} \sim \sum_K \exp(-K^2/2b^2) D^J_{MK}(\theta_i)\chi_K(R, \alpha, \beta_1, \beta_2)\,, \tag{3}$$

where in general, χ_K can be any molecular excitation mode. As for the value of b, we take 1.3, which is consistent with the di-nuclear configuration of ^{28}Si + ^{28}Si system.

2.2. Spin alignments by angular correlations

We define scattering waves and the collision matrix $U_{c'c}$ such as

$$\psi \sim (G_c - iF_c) - \sum_{c'} U_{c'c}(G_{c'} + iF_{c'})\,. \tag{4}$$

By using the R-matrix formula with one level approximation, we obtain $U_{c'c} = e^{-i\phi'_{l'}}(-2\sqrt{2P_{c'l'}}\gamma_{c'l'}\sqrt{2P_{cl}}\gamma_{cl})e^{-i\phi_l}/\Gamma_{\rm total}$ for the inelastic scattering, where the reduced widths γ_{cl} are calculated from the model wave functions. The scattering amplitudes with specified magnetic substates for the mutual 2^+ excitation are given

by

$$X_{m_1m_2}(\mathbf{k}',\mathbf{k}) = \frac{2\pi}{ik} \sum_{L',S',M} (22m_1m_2|S'M'_S)(L'S'm'M'_S|JM) \times i^{J-L'} e^{i(\sigma_J+\sigma'_{L'})} U^J_{L'S'} Y^*_{JM}(\hat{k}) Y_{L'm'}(\hat{k}'), \quad (5)$$

where $\mathbf{k}$ and $\mathbf{k}'$ denote the initial and final relative momenta between the two ^{28}Si nuclei, respectively.

The transition amplitudes for the γ-ray emissions from the polarized nuclei are discussed by several authors (see for example Ref. [8]). For two-photon emissions from the mutual excitation, the amplitudes are given as

$$A^{\sigma_1\sigma_2}_{I_1I_2} = \sum_{m_1m_2} X_{m_1m_2}(\mathbf{k}',\mathbf{k})(00|H_{\sigma_1}|I_1m_1)(00|H_{\sigma_2}|I_2m_2), \quad (6)$$

where the transition matrix elements $(00|H_\sigma|Im) \sim (-1)^{I-m} d^I_{m\sigma}(\theta_\gamma) e^{-im\phi_\gamma}$ describe γ-ray emissions. σ_1 and σ_2 denote right/left-hand circular polarizations of the emitted γ rays, i.e. $\sigma = \pm 1$, and after summing over them the square of the absolute values of Eq. (6), we obtain the γ-ray intensities. In the experiment, only one of the two emitted photons is detected in most cases, even with EUROGAM, and so we take an average over the angles of one photon. Note also that the intensities of the detectors are averaged over the azimuthal angle ϕ_γ in Fig. 2. Thus the angular correlations are expressed as

$$W(\theta_\gamma) = \sum_m P_m W_m(\theta_\gamma), \quad (7)$$

where P_m denote the probabilities in the correlated m magnetic substates of one of the two fragments and are given by $P_m = \sum_{m_2} |X_{mm_2}(\mathbf{k}',\mathbf{k})|^2$. And $W_m(\theta_\gamma)$ denote the E2 γ-ray angular distributions $1/2 \cdot \sum_{\sigma=\pm1} (\sqrt{5/4\pi} d^2_{m\sigma}(\theta_\gamma))^2$ (see for example Ref. [9]).

3. Results and Discussion

We inspect results for two typical molecular states. One is the molecular ground state where all the internal motions are zero-point ones, and another is the butterfly excited state. Theoretical intensities of γ rays emitted by the ^{28}Si fragments in the decay of the molecular ground state ($J = 38$) are given in Fig. 2, indicated by dotted lines, which are seen to be in quite good agreement with the data in all the three axes (a), (b) and (c). Those for the decay of the butterfly excited state are displayed in Fig. 5. A dominant "$m = 2$" substate in the fragment direction is seen in (c), and so the results are much different from the former. One may expect that results for the butterfly mode are favorable for the "$m = 0$" characteristic, because spin orientations are perpendicular to the normal axis. However, more precisely, "$m = 0$" means "symmetric around the normal axis", which is satisfied by neither of excited states such as butterfly nor twisting (not shown here) with a well-defined direction of the spin on the reaction plane.

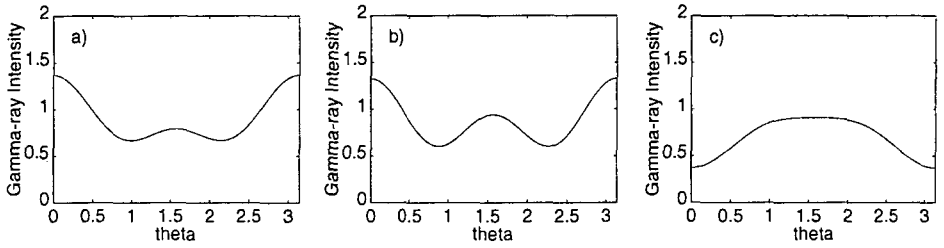

Fig. 5. γ-ray intensities for the angular correlations with three quantization axes, for the butterfly excited state. (a) the z axis in the beam direction, (b) normal to the scattering plane and (c) in the fragment direction.

4. Concluding Remarks

We have examined several molecular modes among which one of them agrees with the characteristic angular correlation data "$m = 0$". None of the normal modes are in agreement with "$m = 0$", because the excited states, such as butterfly and twisting, have specified spin directions, respectively, i.e. "$m = 2$" in their own directions. Only the K-mixed ground state has been selected as a good candidate.

The structure of the K-mixed ground state should be called "wobbling mode", which is due to the triaxial deformation of the ^{28}Si + ^{28}Si stable configuration. K-rotational modes, such as tilting or wobbling, have been discussed for deep inelastic scattering processes [10], but up to now the appearance of the mode in a resonance phenomenon has not been known. As an experimental technique, the angular correlation measurement is a powerful tool for the study of nuclear structures of heavy-ion resonances, and further progress is strongly desired.

Acknowledgement

The authors thank Drs. C. Beck and F. Haas for stimulating discussions in their collaborations.

References

1. R. Nouicer and C. Beck et al., *Phys. Rev.* **C60** (1999) 041303.
2. R.W. Zurmühle, *Proc. Fifth Intern. Conf. on Clustering Aspects in Nuclear and Subnuclear Systems*, Kyoto, July, 1988; *J. Phys. Soc. Jpn.* **58** (1989) Suppl., p. 37; D. Konnerth et al., ibid. 325.
3. E. Uegaki and Y. Abe, *Prog. Theor. Phys.* **90** (1993) 615.
4. E. Uegaki and Y. Abe, *Phys. Lett.* **B340** (1994) 143.
5. E. Uegaki and Y. Abe, *Proc. Fifth Intern. Conf. on Clustering Aspects in Nuclear and Subnuclear Systems*, Kyoto, July, 1988, p. 330; *Phys. Lett.* **B231** (1989) 28.

6. A. Bohr and B.R. Mottelson, *Nuclear Structure*, Vol. II, Benjamin, Massachusetts, 1975, p. 175.
7. Y.R. Shimizu, private communication (in the talk this mode is referred as tilting, but is closer to wobbling); S.W. Ødegård et al., *Phys. Rev. Lett.* **86** (2001) 5866.
8. F. Rybicki, T. Tamura and G.R. Satchler, *Nucl. Phys.* **A146** (1970) 659.
9. J. de Boer et al., *Proc. Intern. School Phys., Enrico Fermi Course LXXVII, Nuclear Structure and Heavy-Ion Collisions*, Elsevier, 1981, p. 655.
10. J. Randrup, *Nucl. Phys.* **A447** (1985) 133c.